INVESTIGATION OF MASS AND HEAT TRANSFER PROCESSES IN BOREHOLE THERMAL ENERGY STORAGE

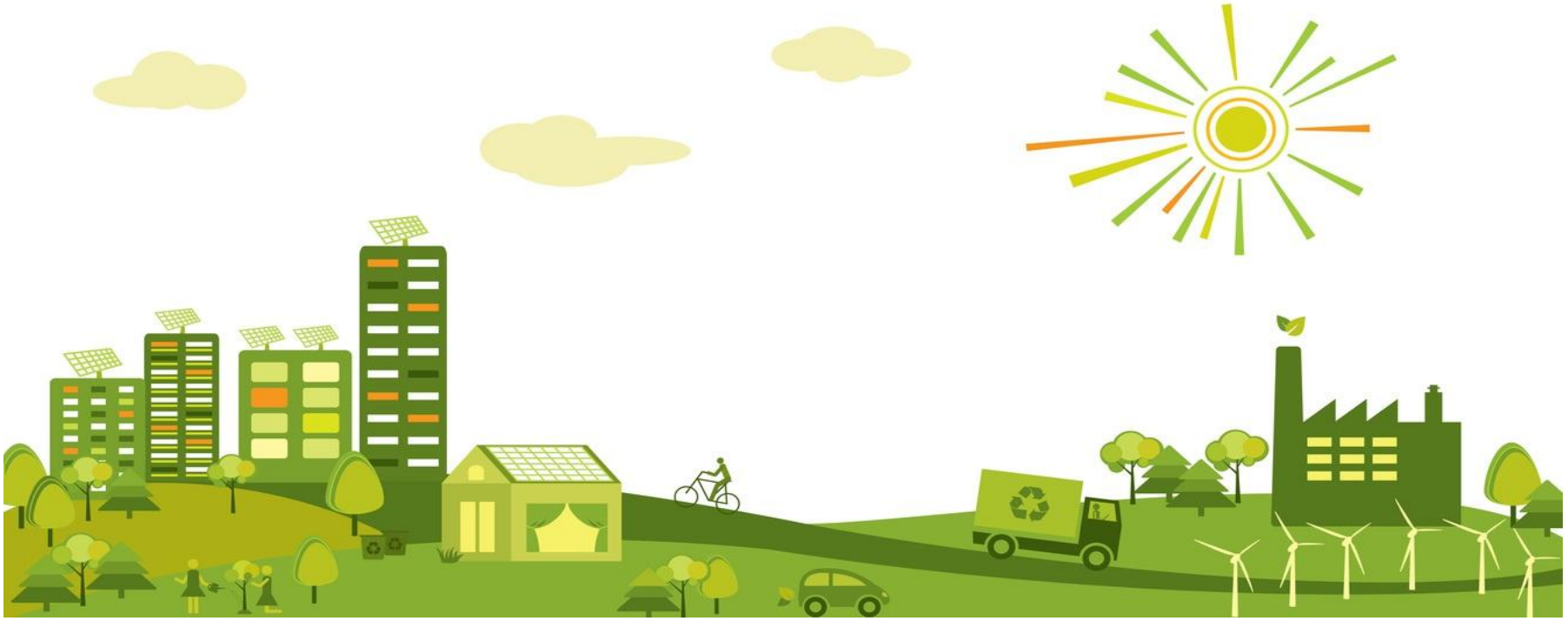

Author: Amanzholov T.E.

Scientific adviser:
Phd, Dr. Lnz Tungatarova M.S.
Phd student Akhmetov B.

Relevance of the research topic: The use of alternative energy sources will significantly reduce the consumption of natural resources currently considered as the main sources of energy, which will make it possible to reduce emissions to the atmosphere and keep the planet clean for future generations. Solar energy is the cleanest source of energy and has great potential for use in heating, ventilation and air conditioning of buildings, etc. Due to natural circumstances, for continuous use of solar energy, an effective heat accumulator is needed, which allows using heat energy regardless of daily and seasonal fluctuations.

Purpose of the work: The purpose of the dissertation is the experimental and numerical study of mass and heat transfer processes in a heat accumulator with borehole heat exchanger.

Task of the study: development of a mathematical model of mass and heat transfer process in a heat accumulator with borehole heat exchanger.

Object of investigation: borehole heat exchanger.

The subject of the study: mass and heat transfer processes in the borehole heat exchanger.

Research methods: experimental methods and mathematical modeling of heat transfer processes in the borehole heat exchanger.

Theoretical and practical significance of the research: the designed and installed design of borehole heat exchanger can be used for determining of thermal properties of the soil, which will be used as storage of solar thermal energy. Determination of soil thermal properties and presence of underground flow plays crucial role in storage of solar thermal energy in the ground.

RENEWABLE ENERGY

According to forecasts of specialists, renewable energy sources-

- hydroelectric power stations,
- windmills,
- solar cells and geothermal energy

soon become the second in the top three energy sources on the planet after coal.

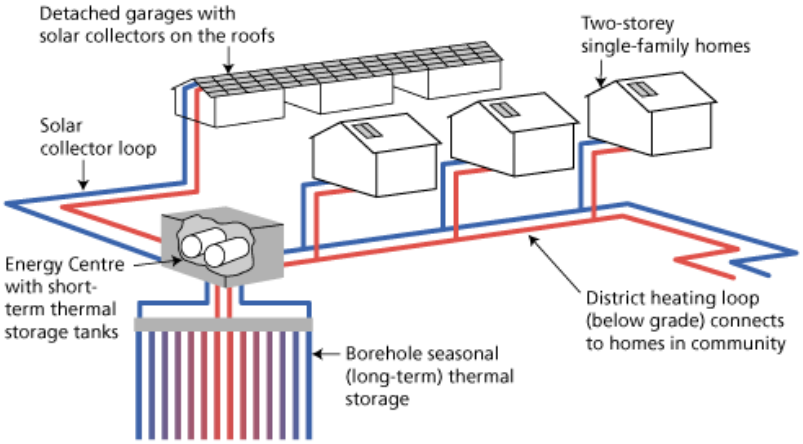

ENERGY STORAGE. BTES SYSTEM

The seasonal thermal energy storage was first offered in the USA in 1960. The main types of seasonal energy storage system:
1) hot water thermal energy storage (HWTES),
2) aquifer thermal energy storage (ATES),
3) gravel-water thermal energy storage (GWTES) and
4) borehole thermal energy storage (BTES).

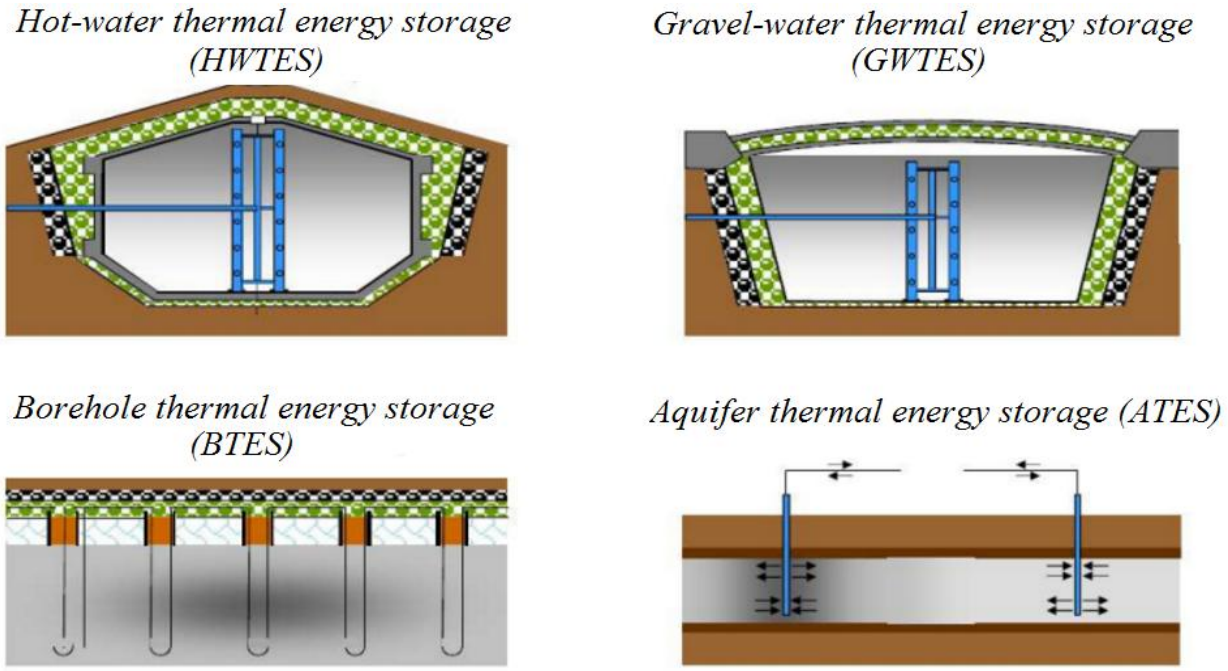

Figure 1 – Seasonal thermal energy storages

ENERGY STORAGE. BTES SYSTEM

The advantages of BTES are the extend ability and the lower effort for construction compared to HWTES and GWTES. The advantages of BTES system are:

- ✓ a relatively compact form of the geothermal energy system;
- ✓ for installation, various type of soils can be used;
- ✓ it is acceptable to use both for active and for passive (natural) cooling and heating;
- ✓ an ideal solution for residential and non-residential buildings;
- ✓ the cost is lower than other systems.

The criteria of building of efficient heat storage systems are:

- ✓ drilled wells with a diameter of 144-170 mm, a depth of 35 m located concentrically at a distance of 2.25 m;
- ✓ the heat carrier must be distributed in such a way that the loss of one branch or ring minimally affects the heat capacity of the system as a whole;
- ✓ all rings and branches start from the center of the BTES system and the heat carrier move from the center to edge of BTES during the charging and vise versa in disharging processes.

BTES SYSTEM. Borehole heat exchangers

There are three different basic structures of borehole heat exchangers are used for BTES systems

1. A single U-shaped BHE consists of two collector pipes, which are connected at the bottom with a U-shaped PE fitting. Thus, in a single U-shaped BHE there is one inlet and outlet flow tube.
2. The double U-shaped borehole heat exchanger consists of four collector pipes, which are connected in the lower part, in pairs of U-shaped PE fitting. Thus, in the double U-shaped collector there are two inlet and outlet flow tubes.
3. Coaxial designates the coaxial arrangement of the axes of three-dimensional elements. Thus, a coaxial borehole heat exchanger is a collector that consists of two collector tubes built into each other (inner pipe and outer pipe). Thus, depending on the use, the inner tube can be used as inlet pipe and outer pipe can be used as outlet pipe or vice versa.

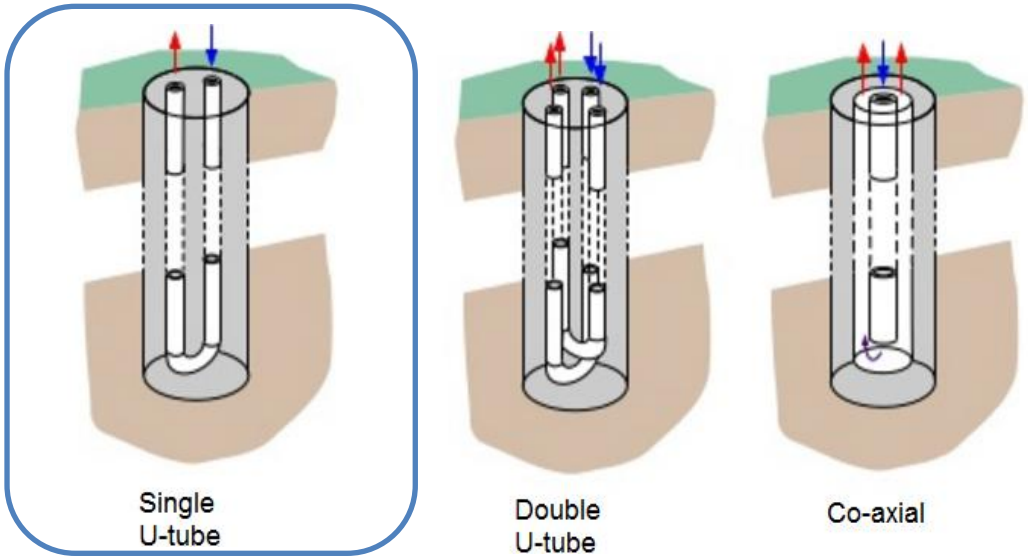

Figure 2 – Basic types of borehole heat exchangers

EXPERIMENTAL STUDIES. **Thermal Response Test (TRT)**

Knowledge of the local geological structure is important for determining the size of the system and the number of inserted borehole heat exchangers. To determine the properties of the soil or to perform thermal response test is necessary to build a device for effectiveness estimating of the BTES system and schematic diagram of which is shown in figure 3.

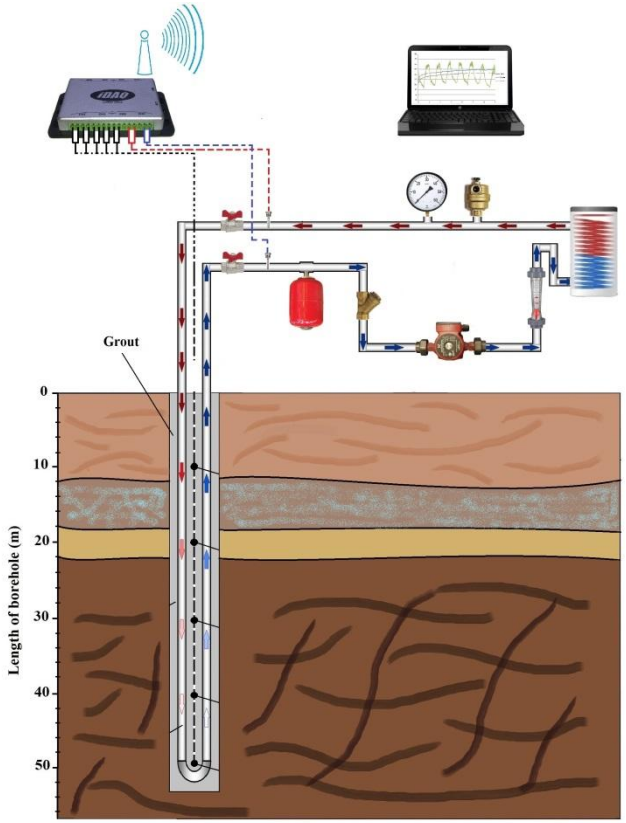

Figure 3 – Schematic diagram of thermal response test installation connected to the vertical ground heat exchanger

EXPERIMENTAL STUDIES. **TRT installation**

With the purpose of development and experimental study of the heat transfer processes in borehole thermal energy storage with a single U-pipe borehole heat exchanger and to evaluate the thermal properties of the ground a special installation is developed for the TRT.

During assembly of the TRT installation, special attention is paid to compact dimensions, performance and the corresponding order of the series-connected parts of the installation, as the carefully assembled system provides accurate measurements of the thermal resistance of the well and effective thermal conductivity of the soil around the well.

Front side

Back side

Figure 4 - Measuring device for carrying out the thermal response test (TRT installation)

EXPERIMENTAL STUDIES. **Analytical model of temperature disturbance in the TRT**

Supplied heat is changed by affection of conduction, convection and radiation heat transfer between heat carrier and environment in distance from TRT rig outlet to BHE inlet and vice versa from BHE outlet to TRT rig inlet and rate of injected heat Q_{BHE} can be written as:

$$Q_{BHE} = Q_{rig} + \underbrace{Q_{amb} + Q_{rad}}_{Q_{d,tot}} \qquad (1)$$

where, Q_{rig} is a generated heat from electrical heater, Q_{amb} is the rate of heat exchange by conduction and convection, Q_{rad} is the rate of heat exchange by radiation. $Q_{d,tot}$ is the sum of Q_{amb} and Q_{rad}

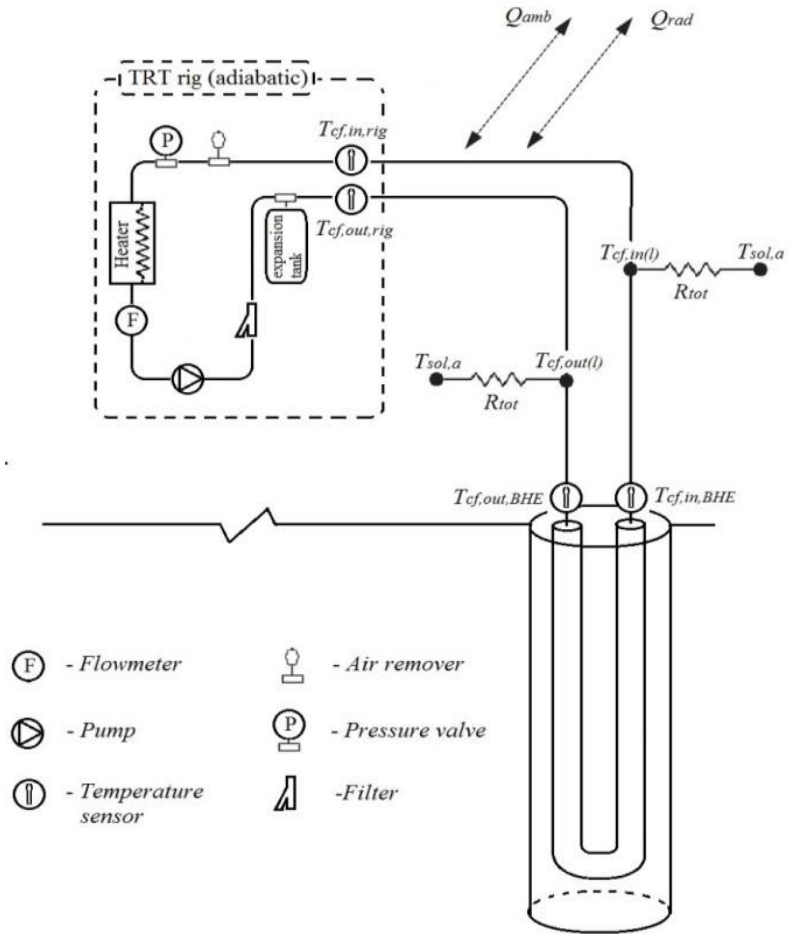

Figure 5- Schematic of the thermal response test installation above the ground

EXPERIMENTAL STUDIES. **Analytical model of temperature disturbance in the TRT**

Changes of temperature in the outflow and inflow circuit along the whole length of connecting pipes can be described as:

$$\Delta T_{cf,out}(t) = T_{cf,out,rig}(t) - T_{cf,out,BHE}(t) \quad (2)$$

$$\Delta T_{cf,in}(t) = T_{cf,in,BHE}(t) - T_{cf,in,rig}(t) \quad (3)$$

Total temperature changes in the circuit above the ground gained from environment can be expressed as:

$$\Delta T_{cf,tot}(t) = \Delta T_{cf,in} + \Delta T_{cf,out} \quad (4)$$

After determining of temperature changes along the whole length of connecting pipes the rate heat exchange between circulating fluid and environment can be defined as:

$$Q_{d,tot}(t) = \rho_{cf} c_{cf} \dot{V}_{cf} \Delta T_{cf,out}(t) \quad (5)$$

$$Q_{d,in}(t) = \rho_{cf} c_{cf} \dot{V}_{cf} \Delta T_{cf,in}(t) \quad (6)$$

$$Q_{d,tot}(t) = Q_{d,out}(t) + Q_{d,in}(t) \quad (7)$$

EXPERIMENTAL STUDIES.
Analytical model of temperature disturbance in the TRT

Fluctuation of temperature in the inflow and outflow part of connecting pipes can be described as:

$$T_{cf,in,BHE}(t) = T_{cf,in,rig}(t)e^{-k_{in}(t)} + T_{sol,a}(t)(1-e^{-k_{in}(t)}) \quad (8)$$

$$T_{cf,out,BHE}(t) = \left(\frac{T_{cf,out,rig}(t) - T_{sol,a}(t)(1-e^{-k_{out}(t)})}{e^{-k_{out}(t)}} \right) \quad (9)$$

where

$$k(t) = \frac{L}{\rho_{cf} c_{cf} \dot{V}_{cf} R_{tot}(t)} \quad (10)$$

and

$$T_{sol,a} = T_{amb} + \frac{a_{ins} I_{sol}}{h_o} \quad (11)$$

EXPERIMENTAL STUDIES.
Solar-air temperature

Temperature fluctuations in the closed loop are taken into account, since the upper and lower side of connecting pipes above the ground caused by direct, diffuse and reflected solar radiation, respectively. To consider all of these impacts of environment is introduced solar-air temperature and general form of solar-air temperature is:

$$T_{sol,a} = T_{amb} + \frac{a_{ins} I_{sol}}{h_o} \qquad (12)$$

where a_{ins} is a absorptivity of foam surface, I_{sol} is the intensity of global solar irradiation, $h_o = 5.7 + 3.8 v_w$ is the overall heat transfer coefficient.

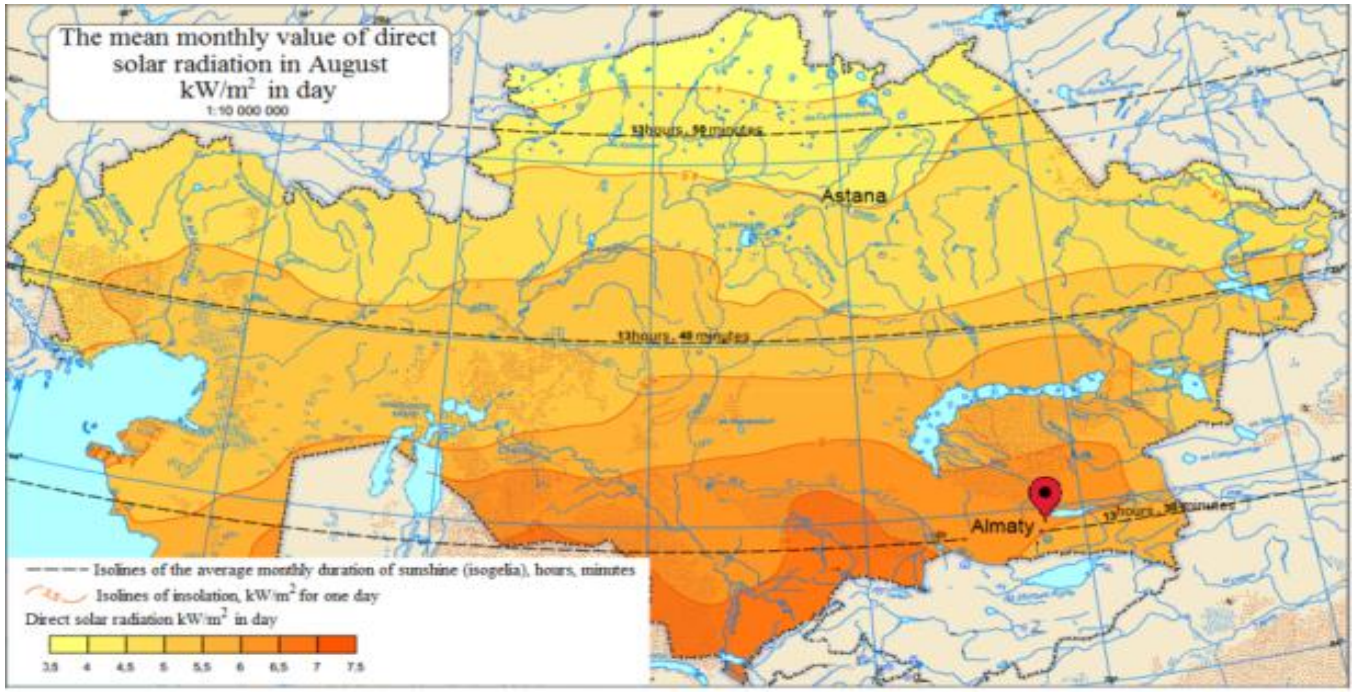

Figure 6- The mean monthly value of direct solar radiation. Kazakhstan

EXPERIMENTAL STUDIES.

Total thermal resistance of connecting pipes

Total thermal resistance of connecting pipes is determined by following equation:

$$R_{tot} = \frac{1}{2\pi r_{p,i} h_i} + \frac{\ln(r_{p,o}/r_{p,i})}{2\pi\lambda_p} + \frac{\ln(1+\tau_{ins}/r_{p,o})}{2\pi\lambda_{ins}} + \frac{1}{2\pi r_{ins,o} h_o} \quad (13)$$

The convective heat transfer coefficient is defined through the Nusselt number (Nu):

$$h_i = \frac{Nu\lambda_{cf}}{2r_{p,i}} \quad (14)$$

Nusselt number depends on velocity of circulating fluid in the closed loop and roughness of pipe surface:

$$Nu = \frac{(f/8)(\mathrm{Re}-1000)\,\mathrm{Pr}}{1+12.7(f/8)^{0.5}(\mathrm{Pr}^{2/3}-1)} \quad (15)$$

Reynolds and Prandtl numbers are approximated as:

$$\mathrm{Re} = \frac{\rho_{cf} v_{cf} 2r_{p.i}}{\mu_{cf}} \qquad \mathrm{Pr} = \frac{\mu_{cf} c_{cf}}{\lambda_{cf}} \quad (16)$$

The Darcy friction factor can be estimated as:

$$f = (0.79\ln \mathrm{Re} - 1.64)^{-2} \quad (17)$$

EXPERIMENTAL STUDIES.
The regression line

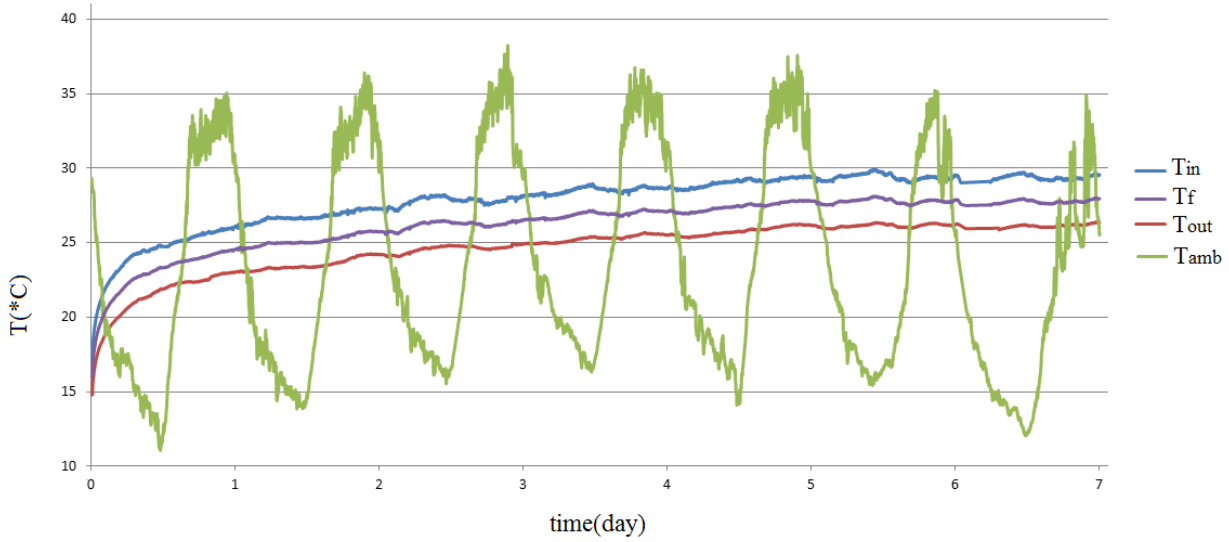

$$T_f(t) = \frac{T_{in}(t) + T_{out}(t)}{2} \qquad (18)$$

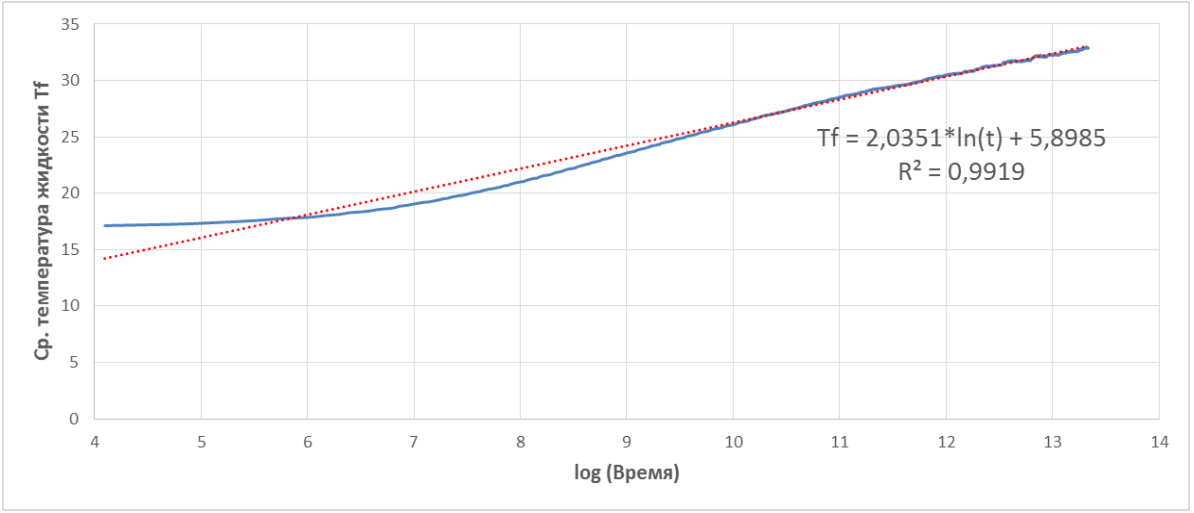

EXPERIMENTAL STUDIES.
Line source model

In line source model is made some assumptions, such as the soil is a homogeneous and isotropic medium and the temperature difference between the inlet and outlet sections of the borehole heat exchanger remains constant over time, the thermal non-stationary problem in the system can be approximately solved by considering a borehole heat exchanger as a linear heat source that instantaneously releases a constant amount of energy in a homogeneous medium (soil), which is unrestricted in the radial direction and has a uniform initial temperature.

Average temperature of circulating liquid:

$$T_f(r_b,t) = T_f(t) \cong \frac{\dot{Q}}{H \cdot 4\pi \cdot \lambda} \ln(t) + \frac{\dot{Q}}{H}\left[\frac{1}{4\pi\lambda}\left(\ln\left(\frac{4\alpha}{r_b}\right) - \gamma\right) + R_b\right] + T_g \qquad (19)$$

or

$$T_f(t) \cong k \ln t + m \qquad (20)$$

where

$$k = \frac{\dot{Q}}{H \cdot 4\pi \cdot \lambda}, \qquad m = \frac{\dot{Q}}{H}\left[\frac{1}{4\pi\lambda}\left(\ln\left(\frac{4\alpha}{r_b}\right) - \gamma\right) + R_b\right] + T_g \qquad (21)$$

A NUMERICAL ANALYSIS

The most common are one U-shaped pipe (consisting of inlet and outlet pipes, which are connected with U-shaped fitting). U-shaped pipe is inserted in the drilled well, which depth constitute 50 meters and filled with mixture of cement and bentonite. A schematic representation of the shape of a single U-shaped pipe is shown in figure. In this work, a shallow closed system consisting of one U-shaped pipe is considered.

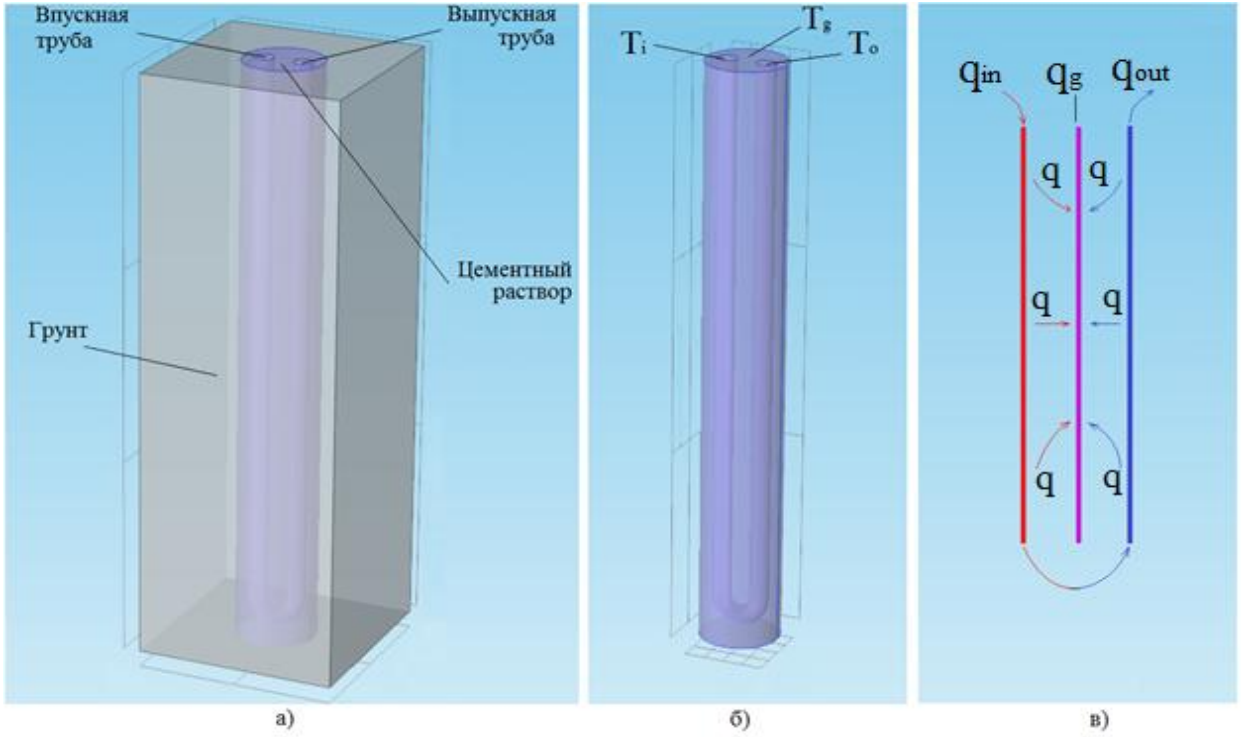

Figure 9 - Schematic representation of one U-shaped heat pipe.

A NUMERICAL ANALYSIS. **Basic equations of the heat flux field in the porous media**

$$\frac{\partial}{\partial x}\left(k_x \frac{\partial h}{\partial x}\right)+\frac{\partial}{\partial y}\left(k_y \frac{\partial h}{\partial y}\right)+\frac{\partial}{\partial z}\left(k_z \frac{\partial h}{\partial z}\right)=0 \qquad (22)$$

где $k_x, k_y, k_z =$ -коффициент филтраци

$$(\rho c)_{eff}\frac{\partial T_s}{\partial t}+(\rho c)_w\left(u\frac{\partial T_s}{\partial x}+v\frac{\partial T_s}{\partial y}+w\frac{\partial T_s}{\partial z}\right)=\frac{\partial}{\partial x}\left((\lambda)_{eff}\frac{\partial T_s}{\partial x}\right)+\frac{\partial}{\partial y}\left((\lambda)_{eff}\frac{\partial T_s}{\partial y}\right)+\frac{\partial}{\partial z}\left((\lambda)_{eff}\frac{\partial T_s}{\partial z}\right)+H \qquad (23)$$

$$\lambda_{eff}=(1-\phi)\lambda_s+\phi\lambda_w \qquad (24)$$

где

$$(\rho C_p)_{eff}=(1-\phi)(\rho C_p)_s+\phi(\rho C_p)_w \qquad (25)$$

A NUMERICAL ANALYSIS. **Heat transfer in vertical ground heat exchanger**

$$(\rho c_p)_w \frac{\partial T_i}{\partial t} + (\rho c_p)_w u \frac{\partial T_i}{\partial z} = \frac{\partial}{\partial z}\left(k_w \frac{\partial T_i}{\partial z}\right) - \frac{2\pi r_o b_{ig}}{A_p}(T_i - T_g) \quad (26)$$

$$(\rho c_p)_w \frac{\partial T_o}{\partial t} - (\rho c_p)_w u \frac{\partial T_o}{\partial z} = \frac{\partial}{\partial z}\left(k_w \frac{\partial T_o}{\partial z}\right) - \frac{2\pi r_o b_{og}}{A_p}(T_o - T_g) \quad (27)$$

$$(\rho c_p)_g \frac{\partial T_g}{\partial t} = \frac{\partial}{\partial z}\left(k_g \frac{\partial T_g}{\partial z}\right) + \frac{2\pi r_o b_{ig}}{A_p}(T_i - T_g) + \frac{2\pi r_o b_{og}}{A_p}(T_o - T_g) - \frac{2\pi r_g b_{sg}}{A_g}(T_g - T_s) \quad (28)$$

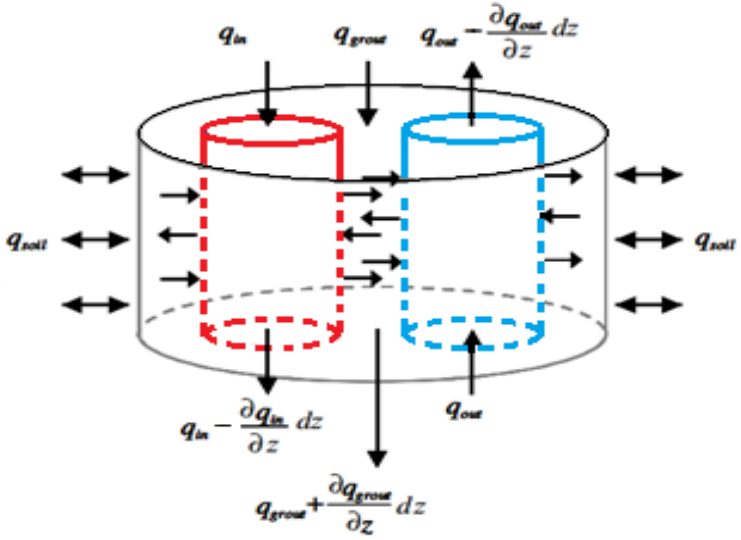

Figure 10 –Heat transfer processes in BHE.

A NUMERICAL ANALYSIS. **Heat transfer in vertical ground heat exchanger**

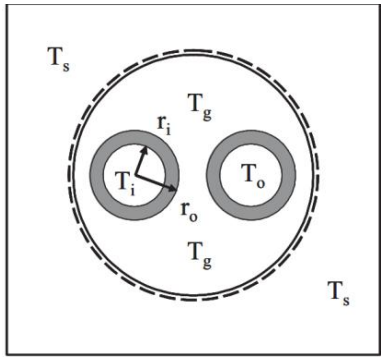

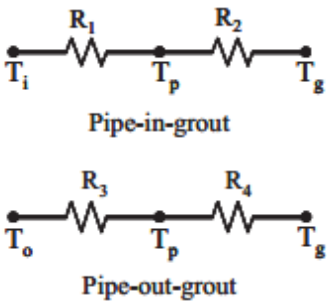

Figure 11 -Temperature resistance between mixture of bentonite and cement and heat carrier.

$$b_{ig} = \frac{1}{R_1 + R_2}, \qquad b_{og} = \frac{1}{R_3 + R_4},$$

$$R_1 = \frac{1}{r_{p,o} / r_{p,o} \cdot h_{in}}, \qquad R_2 = \frac{r_{p,o} \cdot \ln(r_{p,o} / r_{p,i})}{\lambda_p}$$

$$h_{in} = \frac{Nu \lambda_{cf}}{2 r_{p,i}}$$

$$Nu = \frac{(f/8)(\mathrm{Re} - 1000)\,\mathrm{Pr}}{1 + 12.7(f/8)^{0.5}(\mathrm{Pr}^{2/3} - 1)}, \qquad f = (0.79 \ln \mathrm{Re} - 1.64)^{-2}$$

$$\mathrm{Re} = \rho_{cf} v_{cf} 2 r_{p,i} / \mu_{cf} = v_{cf} 2 r_{p,i} / \nu_{cf}$$

$$\mathrm{Pr} = \mu_{cf} c_{cf} / \lambda_{cf}$$

$$\mu_{cf} = 2.44 \times 10^{-5} \times 10^{274.8/(273.15 + T_{cf} - 140)}$$

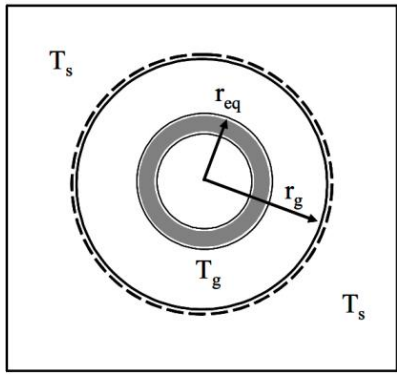

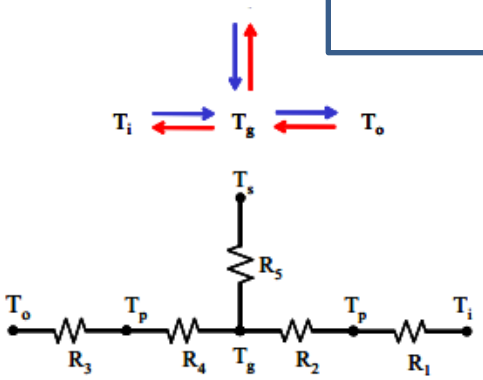

Figure 12 -Temperature resistance between ground and mixture of bentonite and cement.

$$b_{gs} = \frac{1}{\sum R_{ig} + \sum R_{og} + \sum R_{gs}} \qquad R_{gs} = \frac{\ln(r_g / r_{eq})}{2 \cdot \pi \cdot \lambda_g}$$

$$r_{eq} = \sqrt{r_{in}^{\,2} + r_{out}^{\,2}}$$

A NUMERICAL ANALYSIS. **Heat transfer in vertical ground heat exchanger**

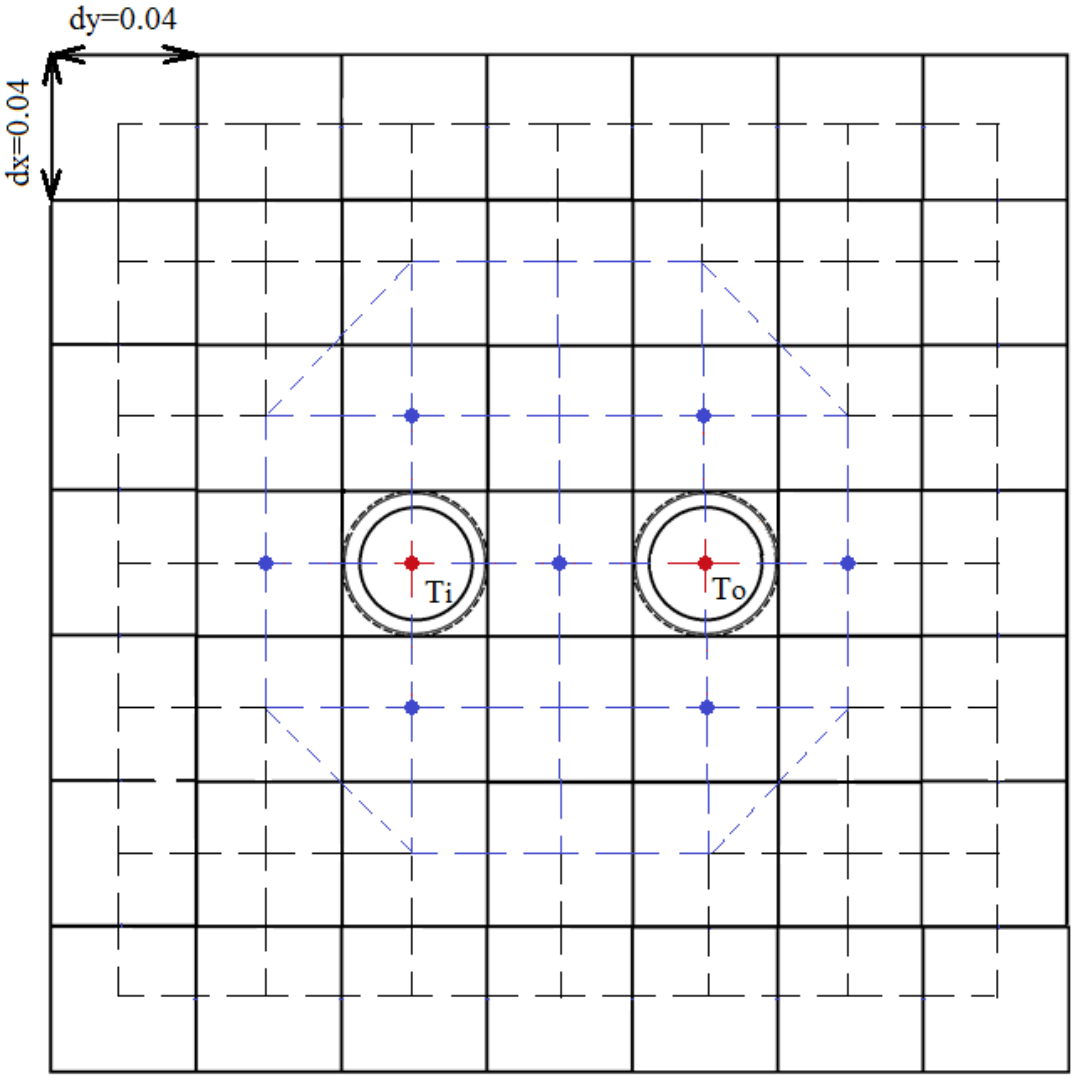

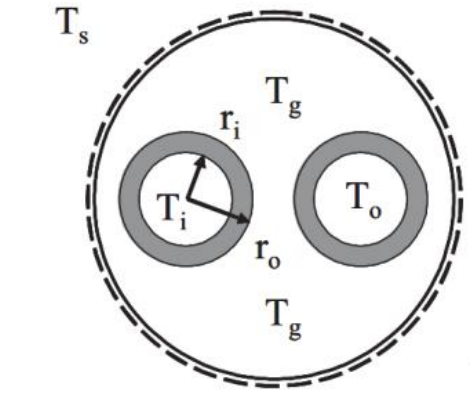

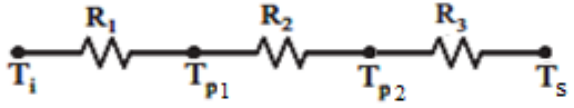

Pipe-in-grout

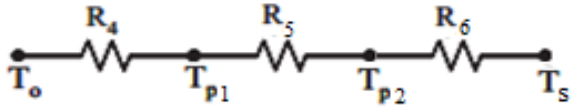

Pipe-out-grout

$$b_{is} = \frac{1}{R_1 + R_2 + R_3}, \qquad b_{os} = \frac{1}{R_4 + R_5 + R_6},$$

A NUMERICAL ANALYSIS.
Initial and boundary conditions

The temperature gradient over the altitude of vertical ground heat exchanger is taken into account to increase the accuracy in the modeling. The initial temperature distribution along the vertical ground heat exchanger was measured before the start of the thermal response test.

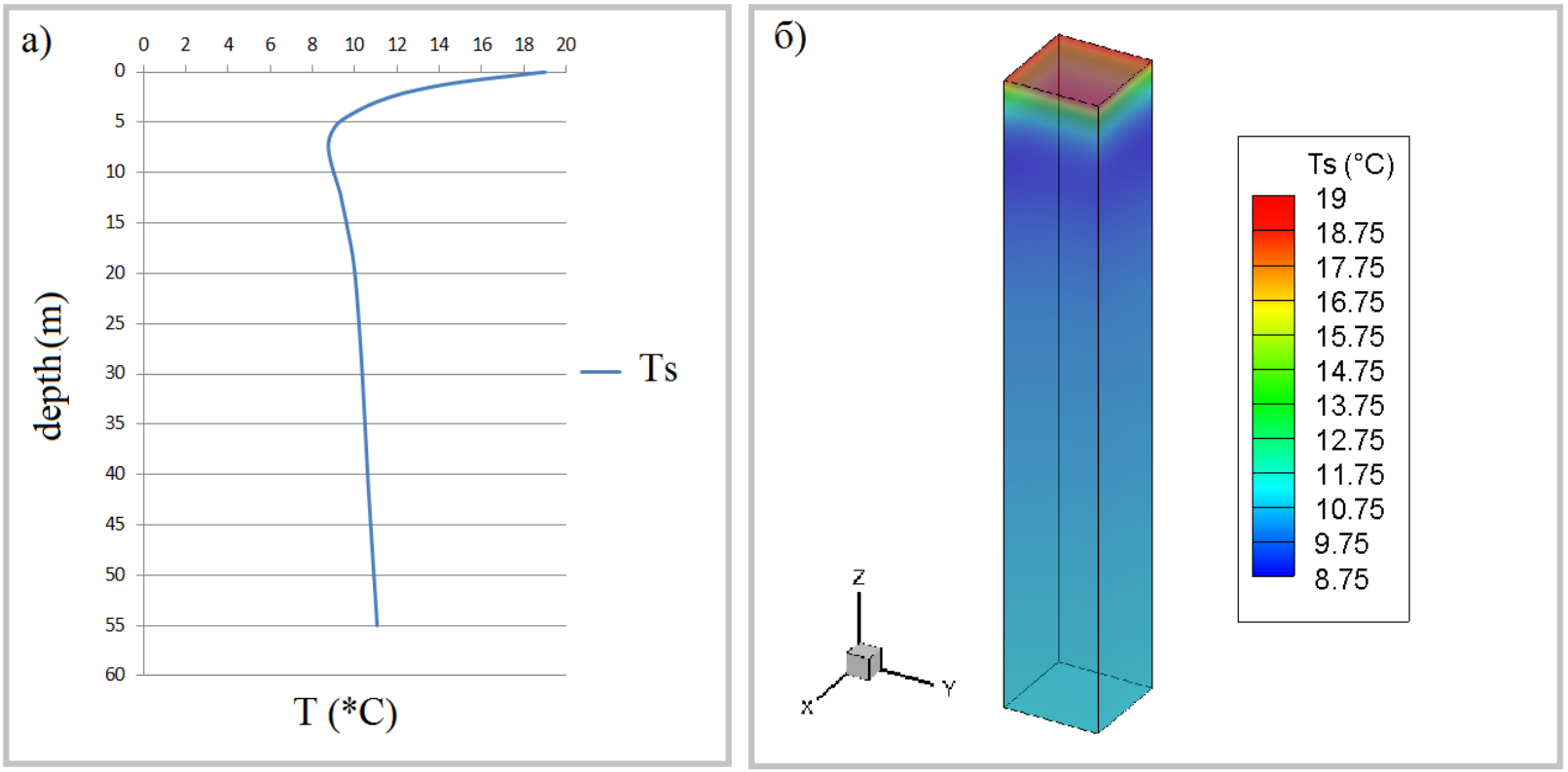

Figure 13 – Initial condition

A NUMERICAL ANALYSIS.
Initial and boundary conditions

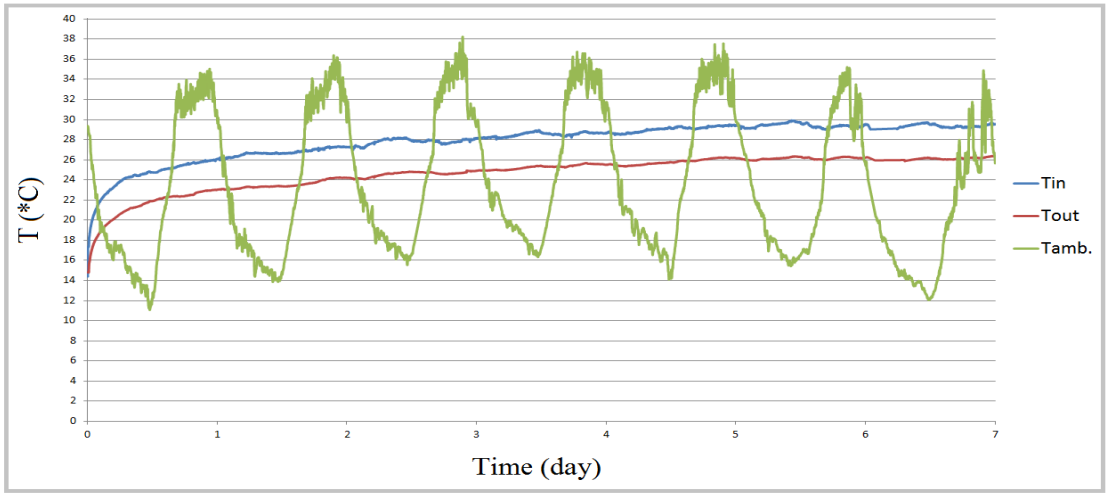

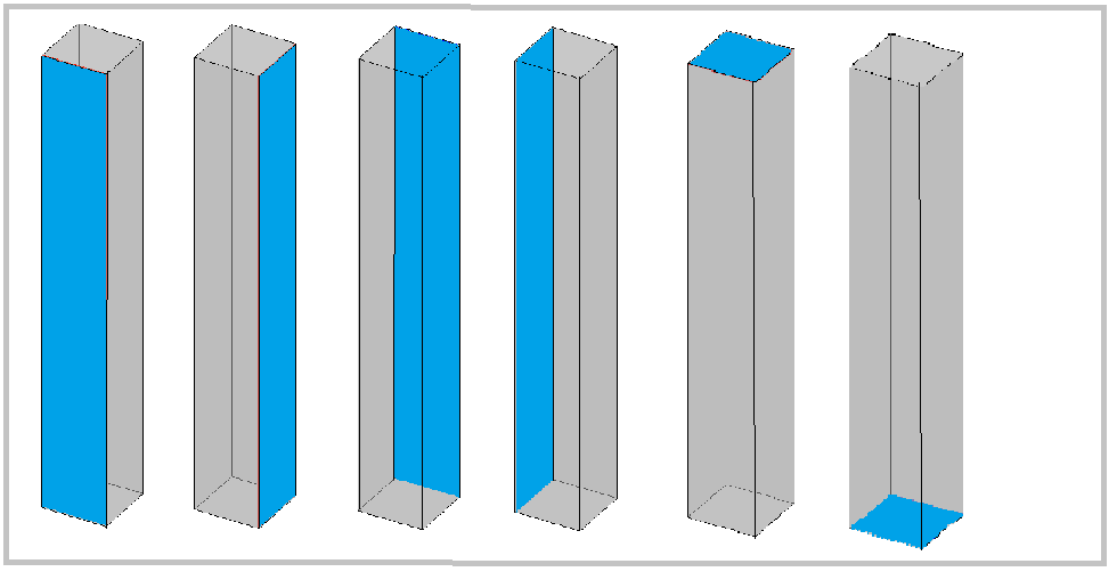

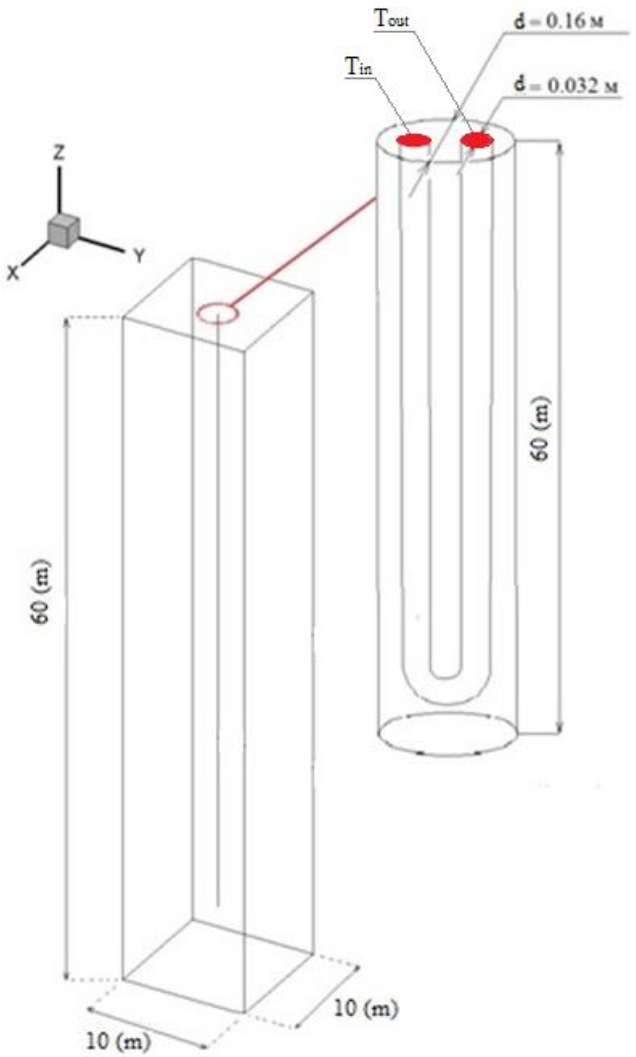

Figure 14 – Boundary conditions

A NUMERICAL ANALYSIS.
Initial and boundary conditions of the soil

Table 6 provides information about layers of the soil around the BHE. The information in the table was used for conducting numerical analysis as well.

Rock type	Depth (meters)	Thermal conductivity (W/m K)	Volumetric heat capacity (MJ/kg K)	Porosity	Hydraulic permeability (m/s)
Loam	0-12	1.8	3.32	0.4	$1.16*10^{-7}$
Coarse sand	12-18	0.83	3.38	0.33	$1.16*10^{-5}$
Clay	18-22	2.33	1.38	0.4	$1.16*10^{-8}$
Fine-grained clayey sand	22-55	1.75	3.19	0.35	$1.16*10^{-6}$

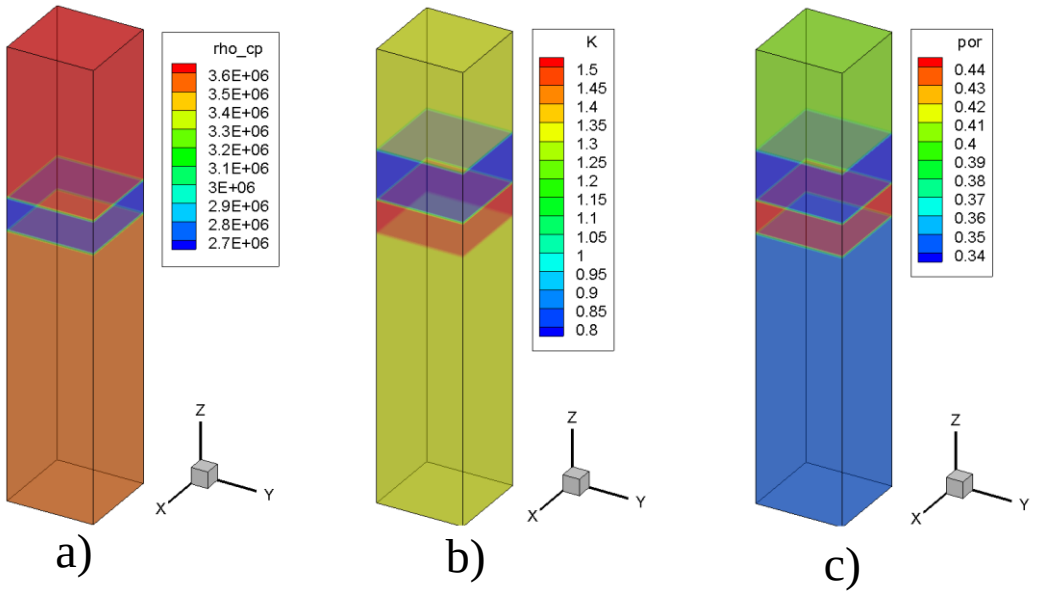

Figure 15 - a)-volumetric heat capacity, b) thermal conductivity and c) porosity of the ground around the borehole heat exchanger.

RESULTS AND DISCUSSIONS. **Heat conductivity test conducted at the Technical University of Sofia - Plovdiv Branch**

RESULTS AND DISCUSSIONS. **Heat conductivity test conducted at the Technical University of Sofia - Plovdiv Branch**

The thermal response test was continued 7 days. The temperature changes along the heat exchanger and the inlet and outlet compartments of the vertical ground heat exchanger during these 7 days are shown in Figure 16. Figure 17 shows the average temperature of the inlet and outlet tubes and the fluctuations of ambient temperature.

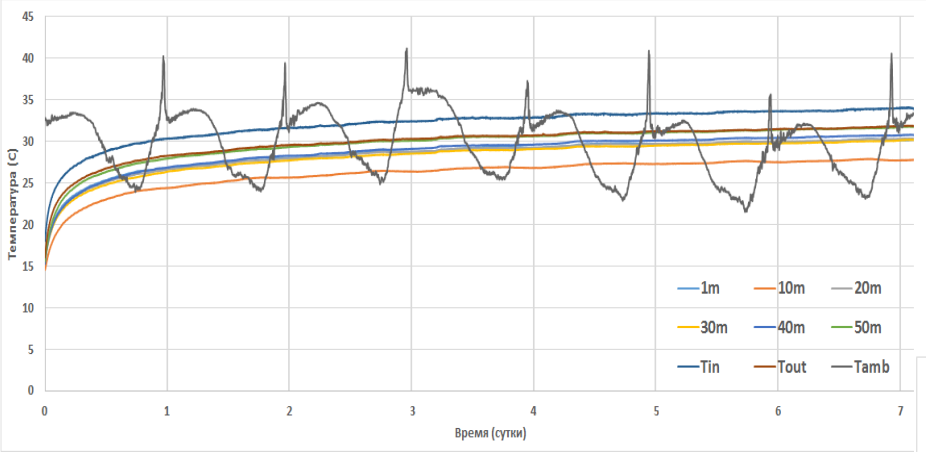

Figure 16 - Temperature data during the thermal response test

Figure 17– Ambient temperature and average temperature of inlet and outlet compartment of the vertical ground heat exchanger tube

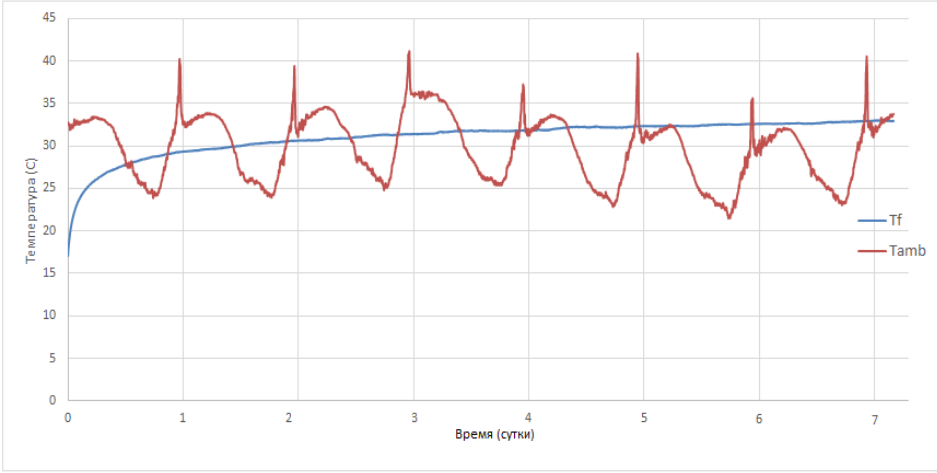

RESULTS AND DISCUSSIONS. **Heat conductivity test conducted at the Technical University of Sofia - Plovdiv Branch**

To use the experimental data to determine the thermal conductivity and thermal resistance, it is necessary to interpolate the middle part of the input and output sections of the vertical ground heat exchanger (Figure 18).

The function found (Figure 18) can not be used in the line source model, since it does not describe the change in mean temperature poorly.

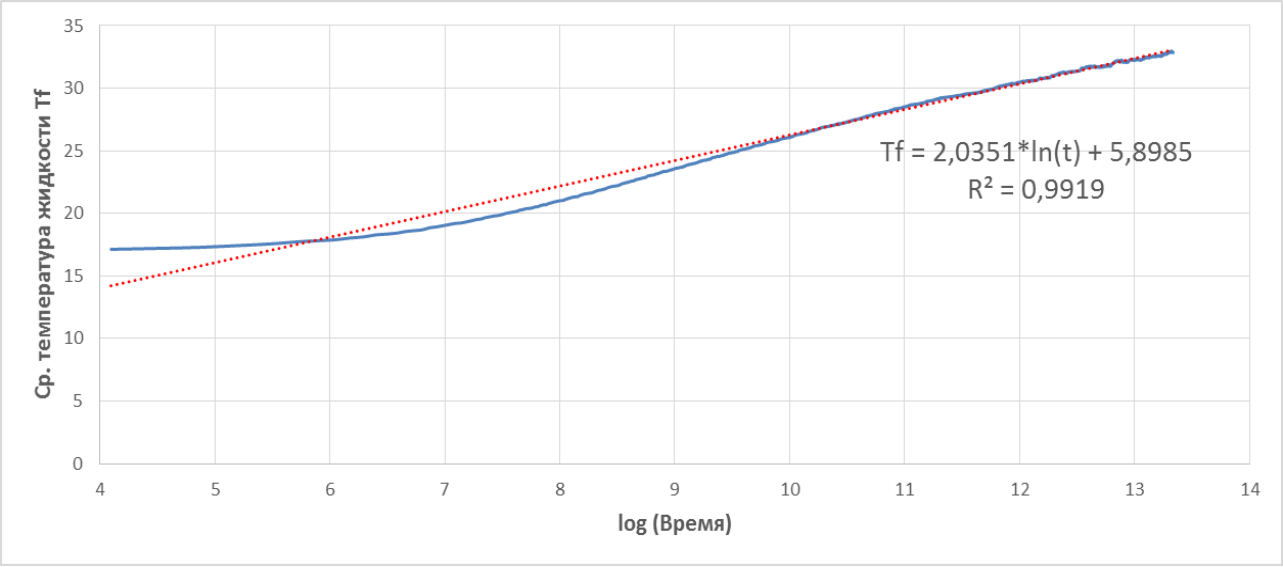

Figure 18 - The regression line (full time)

RESULTS AND DISCUSSIONS. **Heat conductivity test conducted at the Technical University of Sofia - Plovdiv Branch**

The error in approaching the interpolated function to the mean temperature of the liquid is high. In connection with this, the first 10 hours of the experiment are not taken into account when calculating this function. The results of interpolation without taking into account the first 10 hours are shown in Figure 19.

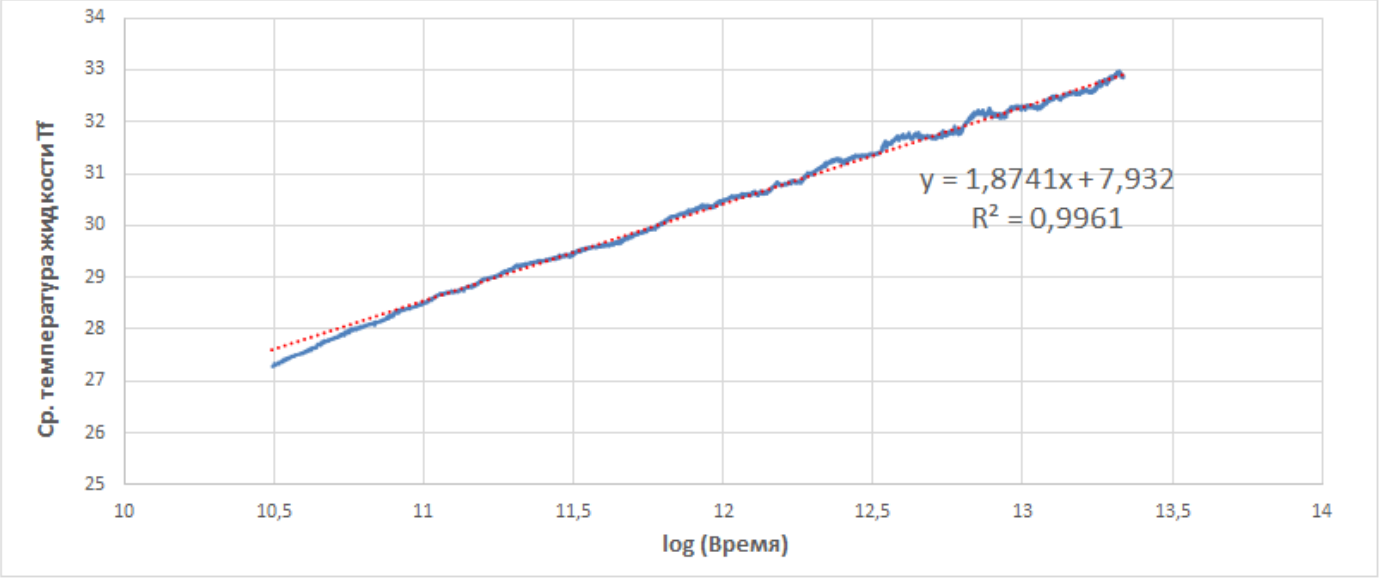

Figure 19 - Regression line without the initial 10 hours

RESULTS AND DISCUSSIONS. **Heat conductivity test conducted at the Technical University of Sofia - Plovdiv Branch**

Deviations at the beginning of the experiment are also observed, and interpolations were carried out without the first 24 hours of the experiment (Figure 20).

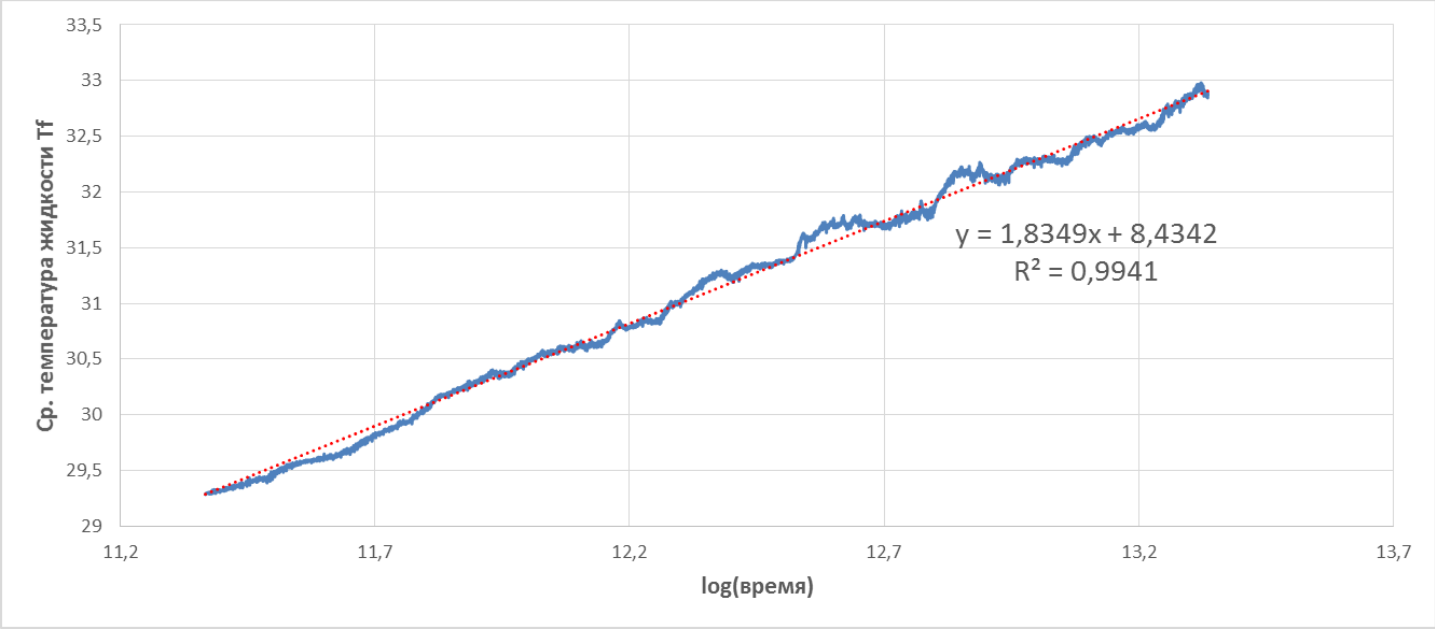

Figure 20 - Regression line without the initial 24 hours

RESULTS AND DISCUSSIONS. **Heat conductivity test conducted at the Technical University of Sofia - Plovdiv Branch**

As a result of the study, a technique for measuring soil properties, in particular, the coefficient of thermal conductivity and thermal resistance of the soil has been worked out.

Table 1 - Results of TRT carried out at the Technical University of Sofia, Plovdiv Branch, Bulgaria

Time	k	m	Q [J/s]	λ [W/mK]	Rb [K/W]
10h	1,87	7,932	1549,53	1,315913	0,249937
1day	1,8349	8,4342	1549,53	1,344026	0,250099
2day	1,7716	9,2597	1549,53	1,392049	0,250072
Mean				1,31	0,24

RESULTS AND DISCUSSIONS. **Heat conductivity test conducted at the Agro-Bio Center of Al-Farabi Kazakh National University, Almaty**

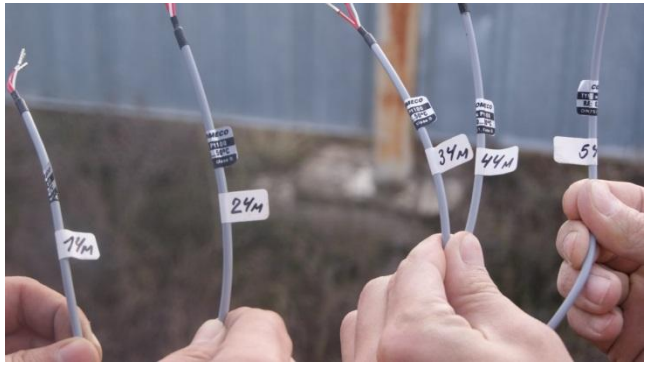

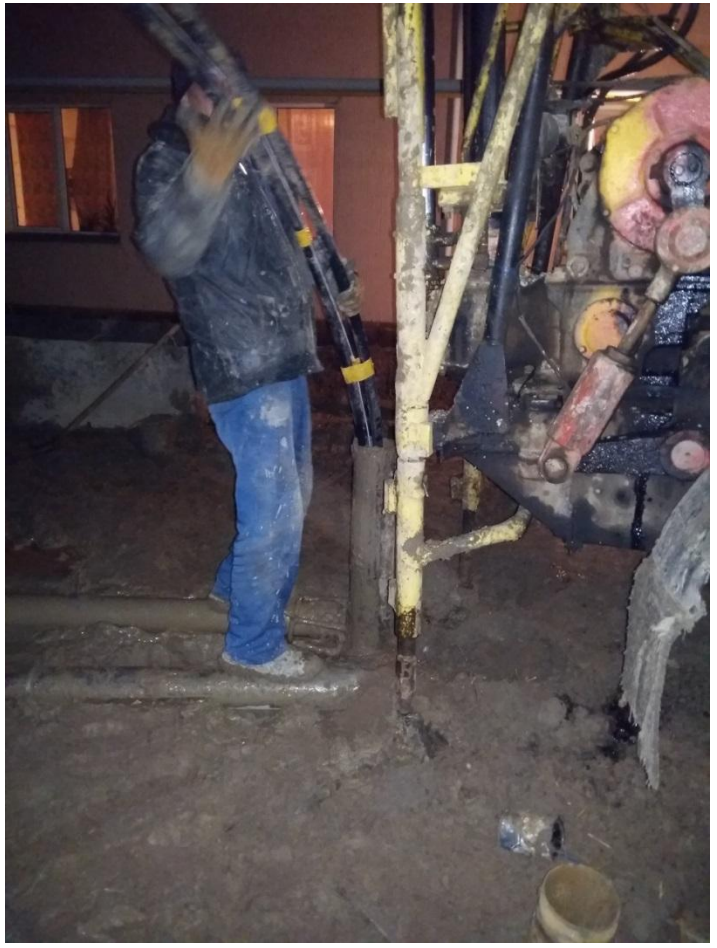

RESULTS AND DISCUSSIONS. **Heat conductivity test conducted at the Agro-Bio Center of Al-Farabi Kazakh National University, Almaty**

Thermal response test was carried out on August in 2016 in the surrounding area of Almaty. Test was continued 7 days. Temperature sensors were installed at the inlet and outlet part of TRT installation and along the borehole heat exchanger every 10 meters. Before the starting TRT, the initial depth depending temperature was measured with helping of temperature sensors installed along the borehole heat exchanger every 10 meters.

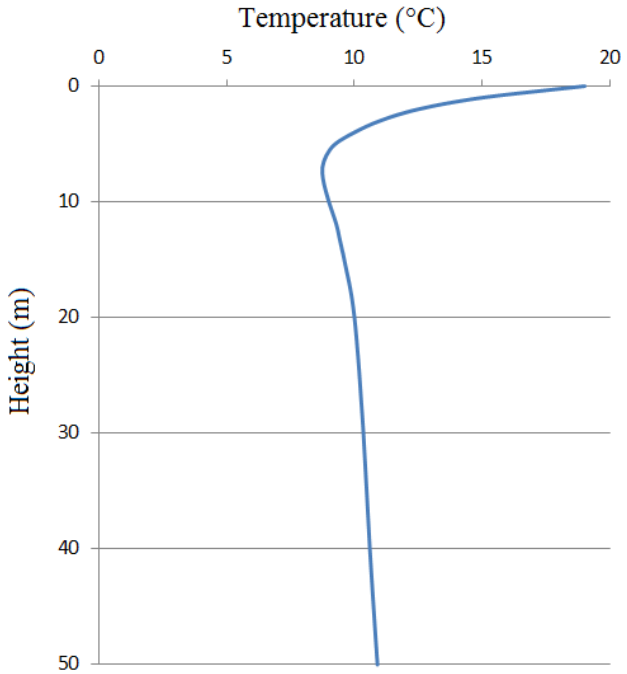

Figure 21 - Initial temperature of the ground

Figure 1 – Initial temperature of the ground around the borehole

EXPERIMENTAL STUDIES. **Solar-air temperature**

Thermal response test carried out in Almaty [43° 15'24"n.l., 76° 55'42"e.l.] for investigation heat transfer processes in BTES. In Almaty direct solar radiation falls are high in the end of summer and it affects to the circulating fluid temperature in the connecting pipes above ground. The average velocity of wind during the thermal response test was 2 m/s

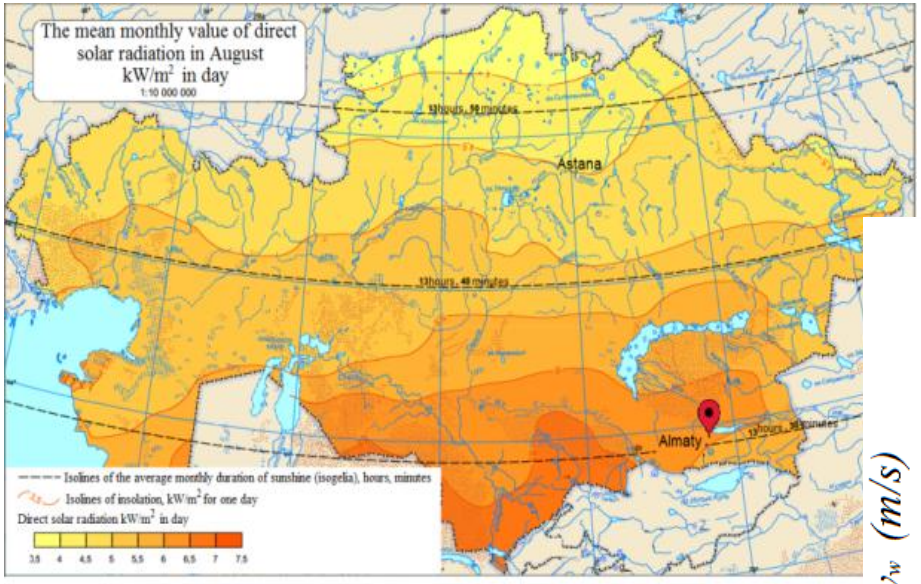

Figure 22 – The mean monthly value of direct solar radiation

Figure 23 – Average wind velocity

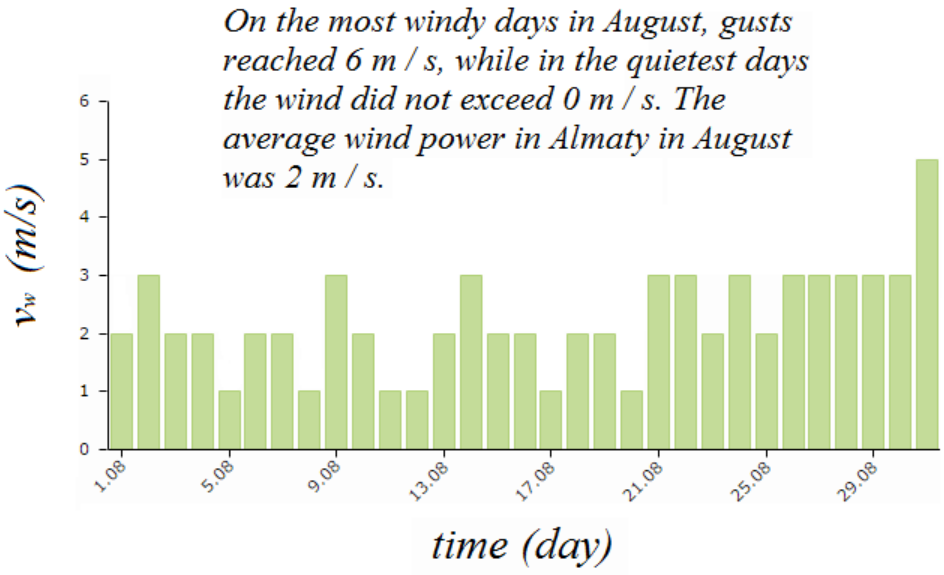

RESULTS AND DISCUSSIONS. **Heat conductivity test conducted at the Agro-Bio Center of Al-Farabi Kazakh National University, Almaty**

The perturbations of temperature were recorded by data logger every 60 seconds and illustrated in figure. There are six temperature fluctuations are illustrated, five of them are temperature fluctuations by depth and last one is ambient temperature fluctuation. Ambient temperature sensor was installed in the TRT installation, therefore there are level of temperature is very high.

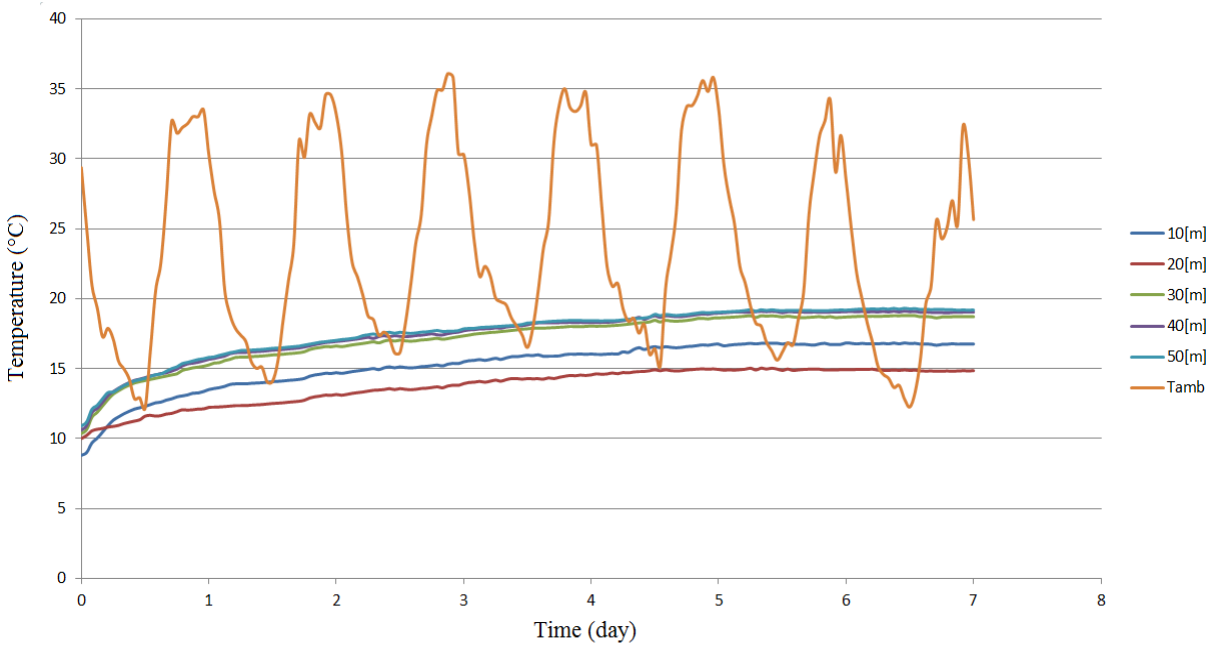

Figure 24 – Temperature perturbation along the borehole heat exchanger during the TRT

RESULTS AND DISCUSSIONS. **Heat conductivity test conducted at the Agro-Bio Center of Al-Farabi Kazakh National University, Almaty**

Also, inlet and outlet temperature was measured. Figure 25 shows inlet, outlet and average temperatures and the fluctuations of ambient temperature.

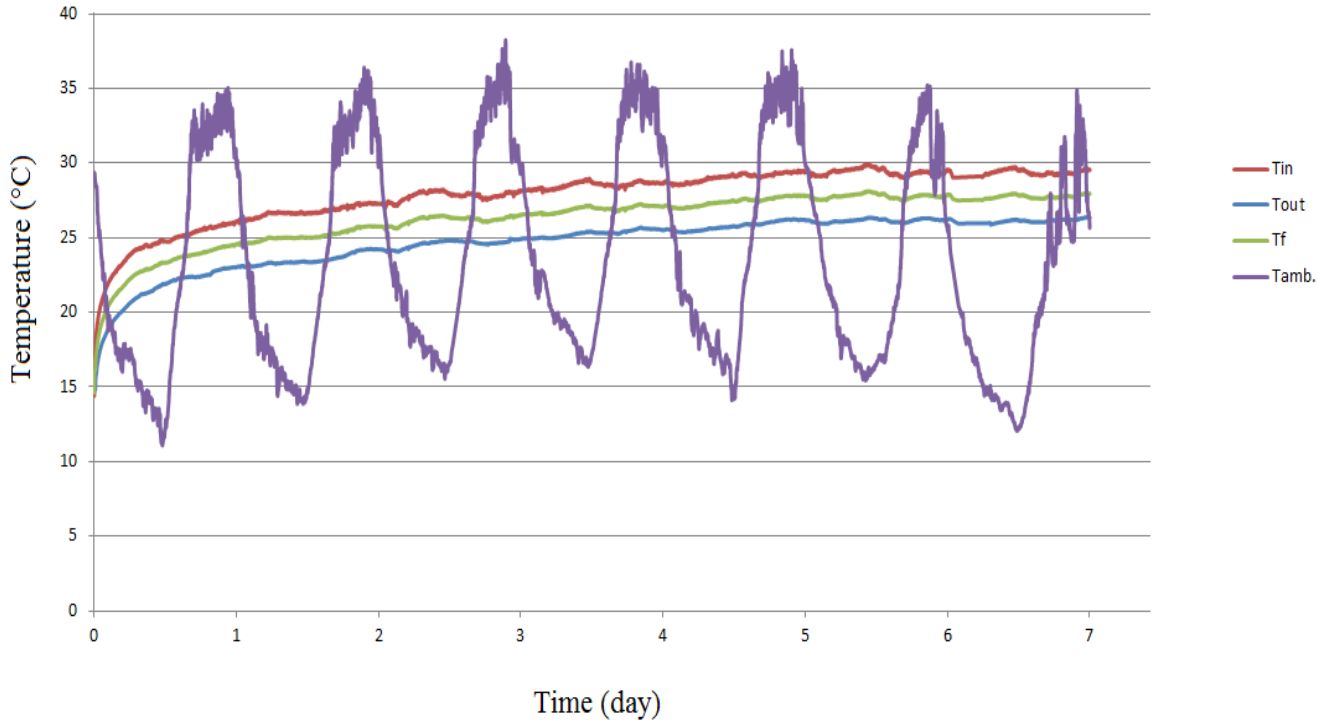

Figure 25 – Temperature perturbation at the inlet and outlet part of BHE

RESULTS AND DISCUSSIONS. **Heat conductivity test conducted at the Agro-Bio Center of Al-Farabi Kazakh National University, Almaty**

To determine the thermal conductivity and thermal resistance of the ground was build the regression line for full time (Figure 26).

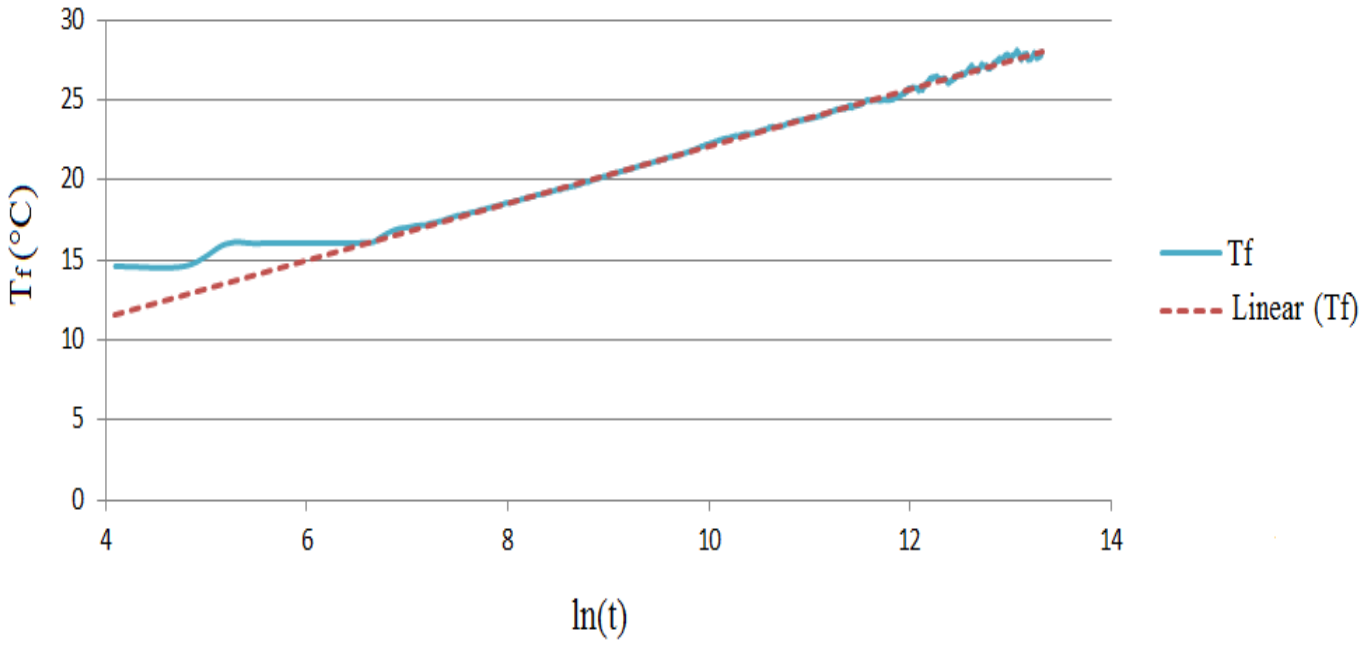

Figure 26 – Regression line for full time

RESULTS AND DISCUSSIONS. **Heat conductivity test conducted at the Agro-Bio Center of Al-Farabi Kazakh National University, Almaty**

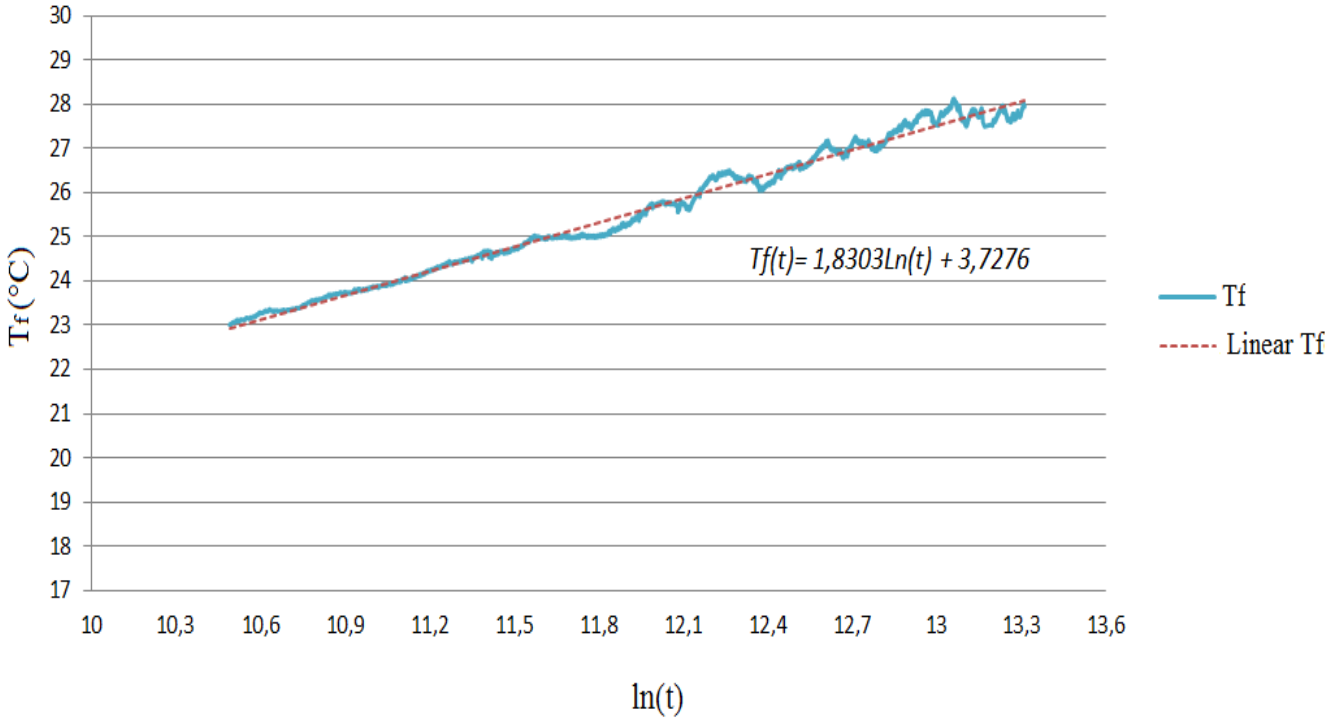

Figure 27 – Regression line without 10 hours

RESULTS AND DISCUSSIONS. **Heat conductivity test conducted at the Agro-Bio Center of Al-Farabi Kazakh National University, Almaty**

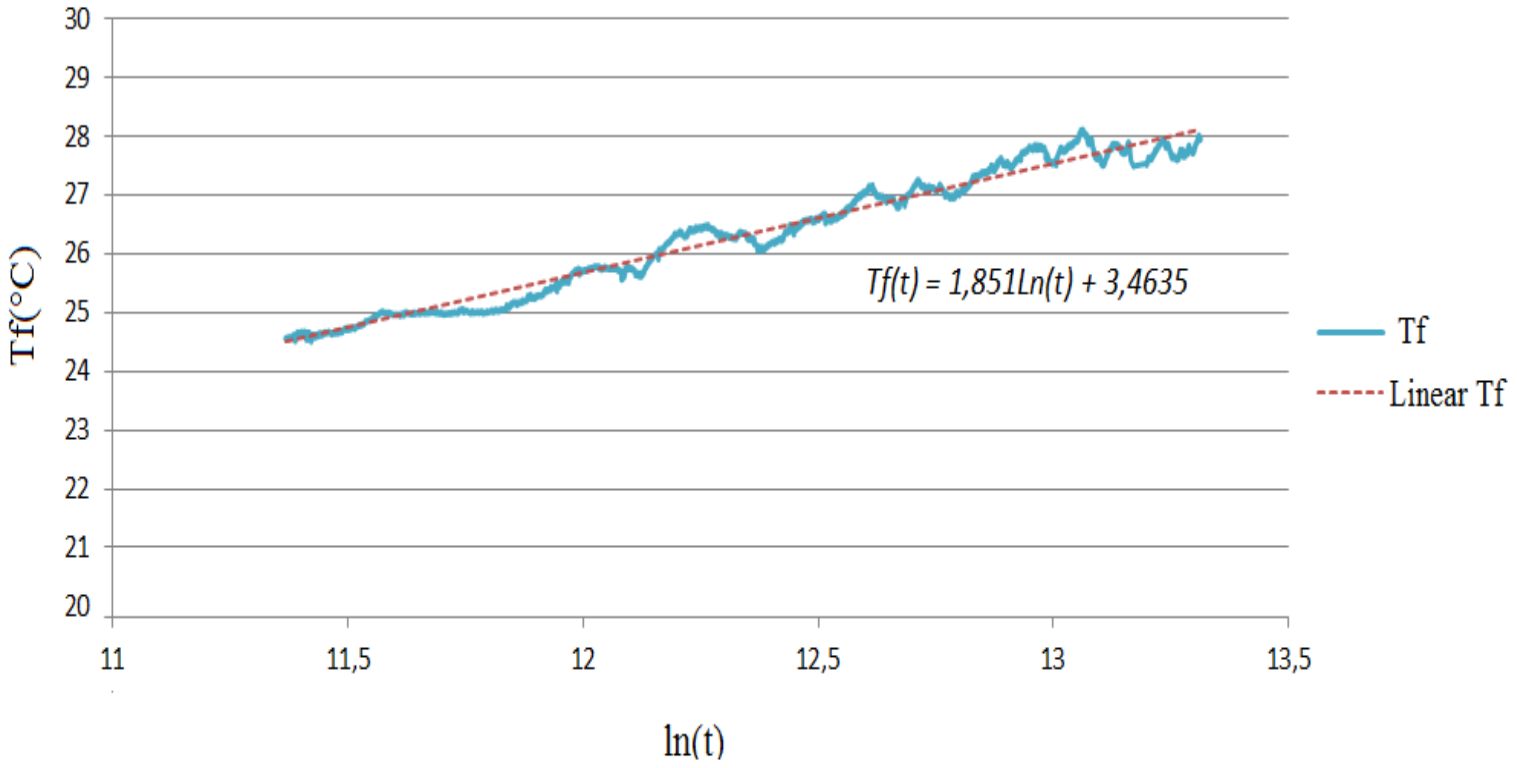

Figure 28 – Regression line without 24 hours

RESULTS AND DISCUSSIONS. **Heat conductivity test conducted at the Agro-Bio Center of Al-Farabi Kazakh National University, Almaty**

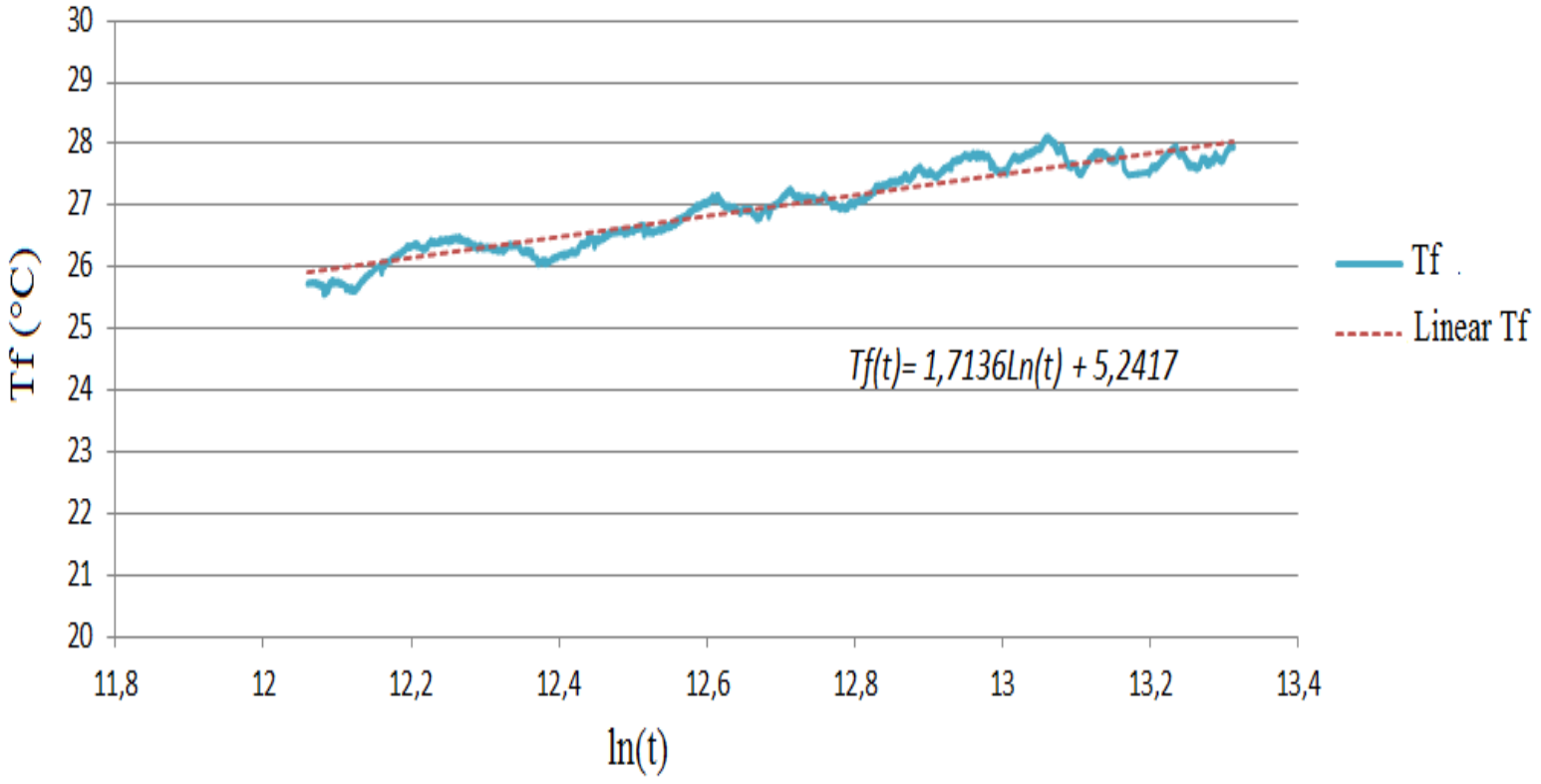

Figure 29 – Regression line without 48 hours

RESULTS AND DISCUSSIONS. **Heat conductivity test conducted at the Agro-Bio Center of Al-Farabi Kazakh National University, Almaty**

The thermal conductivity and thermal resistance coefficients were calculated taking into account the temperature perturbation in the connecting pipes above the ground

Table 2 - Detailed information of rock layers around the borehole in surrounding area of Almaty

Time	k	m	Q [J/s]	λ [W/mK]	Rb [K/W]
10th hour	1,83	3,7276	1924,845	1,674610615	0,207741267
1st day	1,851	3,4635	1924,845	1,655883203	0,205710277
2nd day	1,7136	5,2417	1924,845	1,788655351	0,219845643
Mean				1,71	0,21

RESULTS AND DISCUSSIONS. Numerical results

When drilling the borehole, the presence of the aquifer was noticed around 12-18 m depth. This is also confirmed by the significant decrease of the temperature gradient at the near 20th meter, which is due to the groundwater. In the modelling, the thickness of the groundwater layer was taken as 6 m. And velocity of the groundwater flow was calculated, which is quite reasonable for most of the time (Figure 30).

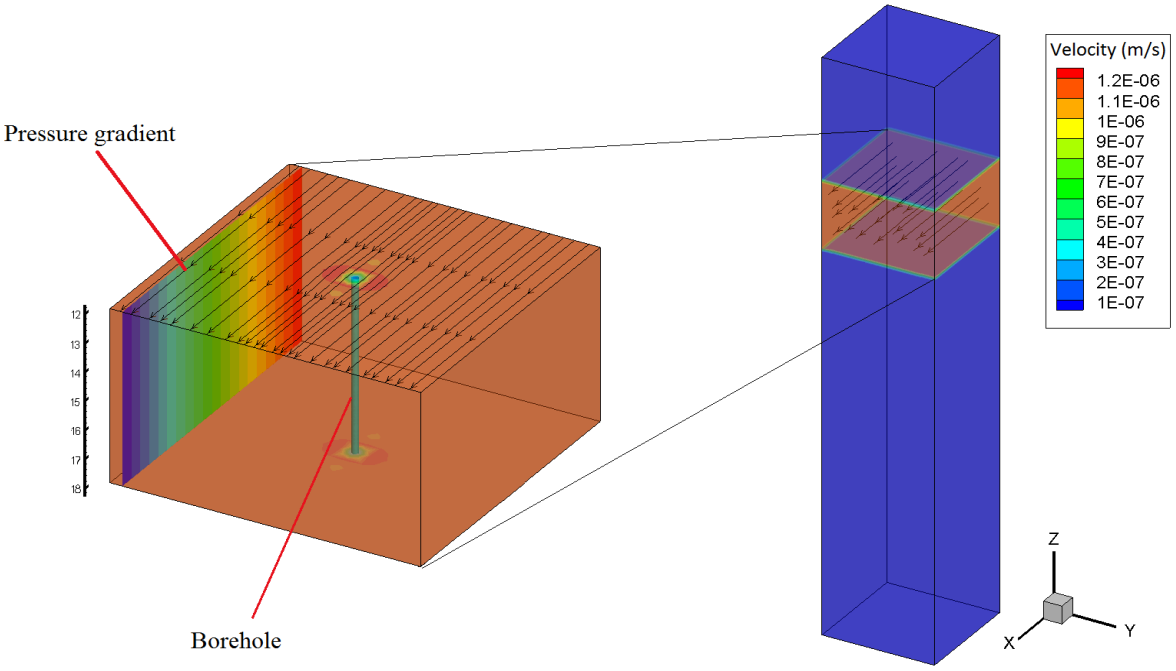

Figure 30 – Underground flow

RESULTS AND DISCUSSIONS. Numerical results

In particular, the temperature data at inlet compartment of the tube (Figure 20) were used as a boundary condition in the simulation and temperature data in the outlet compartment of the tube was computed on the basis of the improved mathematical model. Results of computation represented in figure 30.

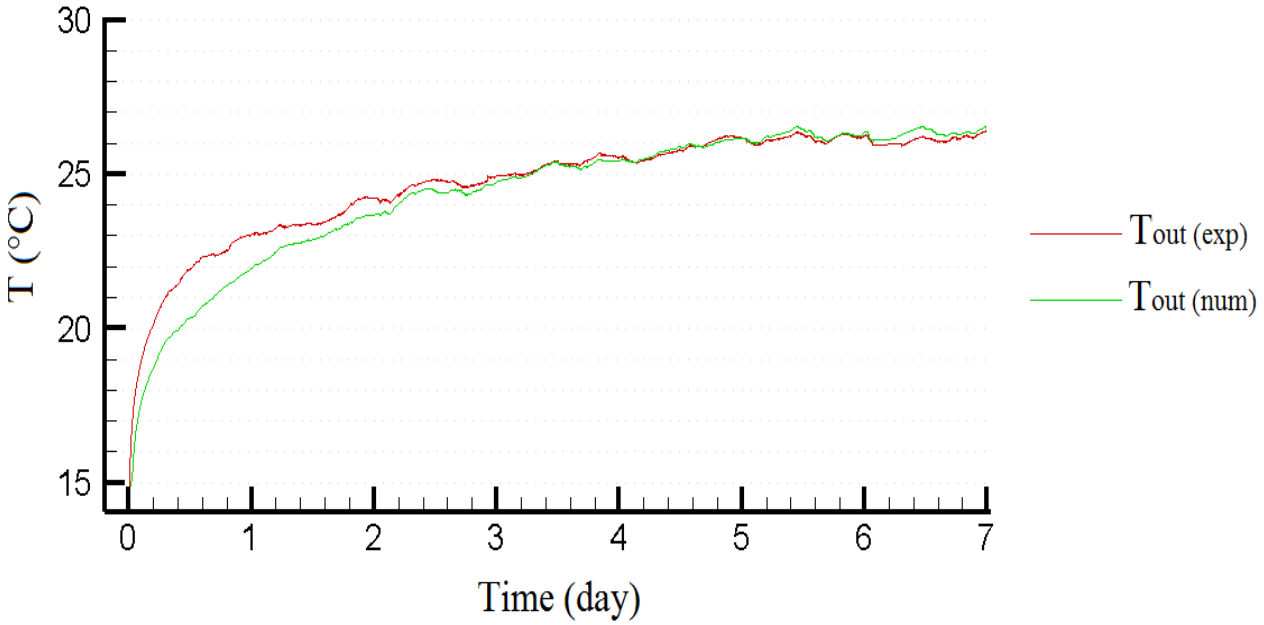

Figure 30 – Comparative chart of experimental and numerical results of measurements at the outlet part of a borehole heat exchanger

RESULTS AND DISCUSSIONS. Numerical results

Temperature distribution in the circumference of the vertical ground heat exchanger during the thermal response test is shown in figure 31.

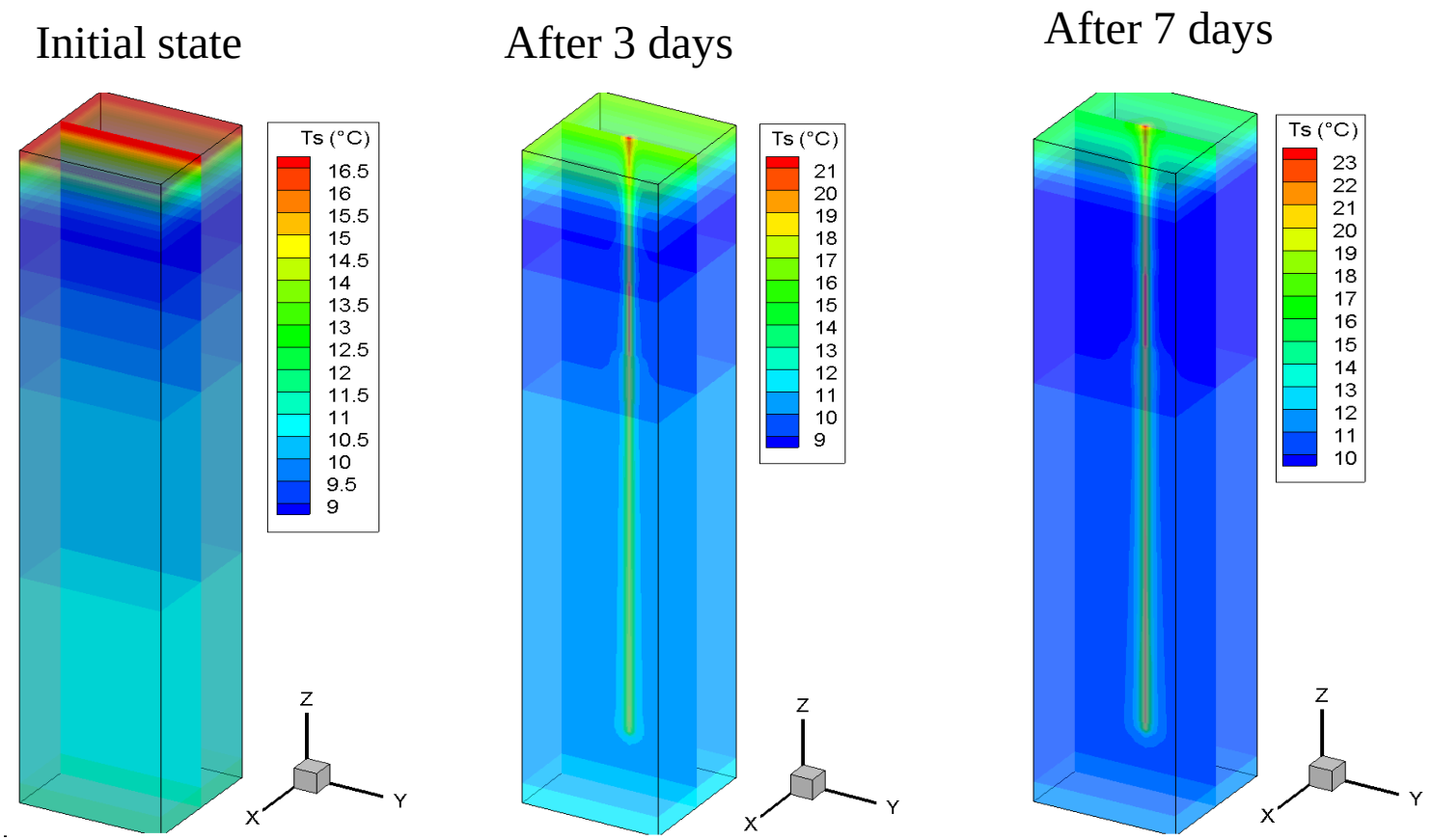

Figure 31 - Temperature field around vertical ground heat exchanger for different times with taking into account the temperature gradient and aquifer

RESULTS AND DISCUSSIONS. Numerical results

Temperature distribution in the circumference of the vertical ground heat exchanger during the thermal response test is shown in figure 31.

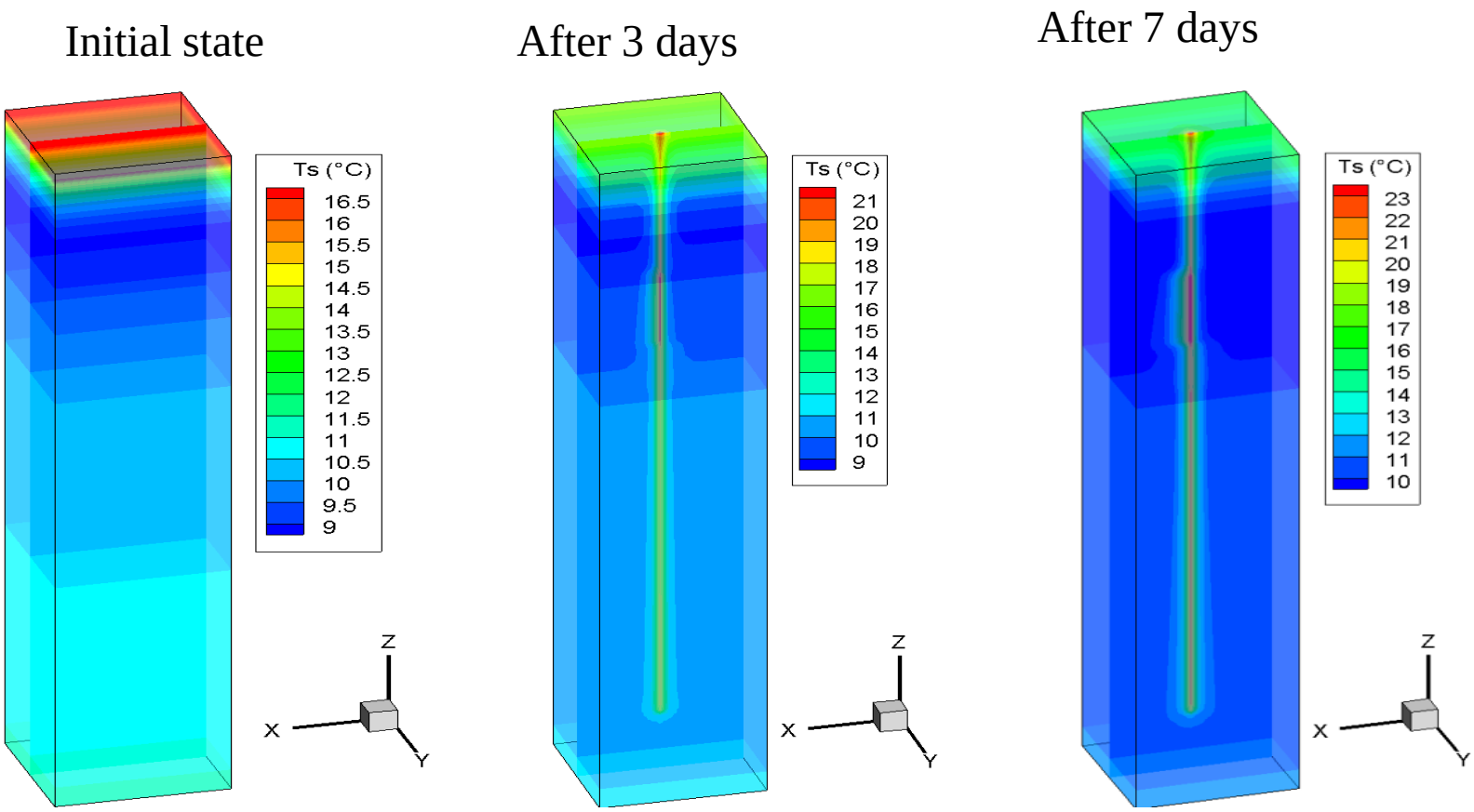

Figure 31 - Temperature field around vertical ground heat exchanger for different times with taking into account the temperature gradient and aquifer

RESULTS AND DISCUSSIONS. Numerical results

Temperature distribution in the circumference of the vertical ground heat exchanger during the thermal response test is shown in figure 31.

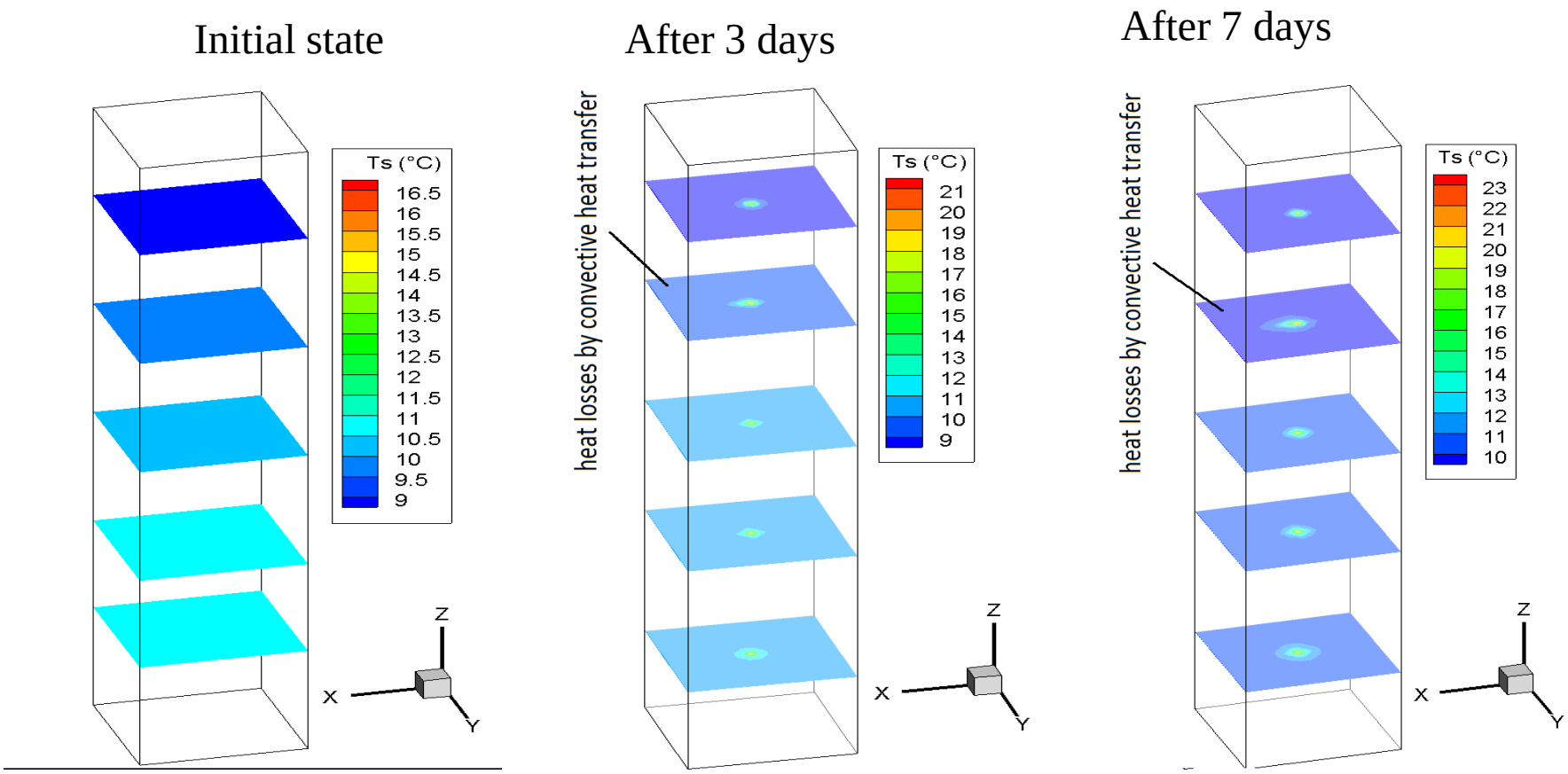

Figure 31 - Temperature field around vertical ground heat exchanger for different times with taking into account the temperature gradient and aquifer

RESULTS AND DISCUSSIONS. Numerical results

In numerical studies, charging of one borehole heat exchanger was also considered. Charging was continued 6 months during the summer and inlet temperature was set 65°C (const.). In this study takes into account an aquifer, which velocity of underground flow is 10cm per day. Such studies give opportunity to estimate the distance length of between borehole heat exchangers in BTES system (Figure 32).

Initial state

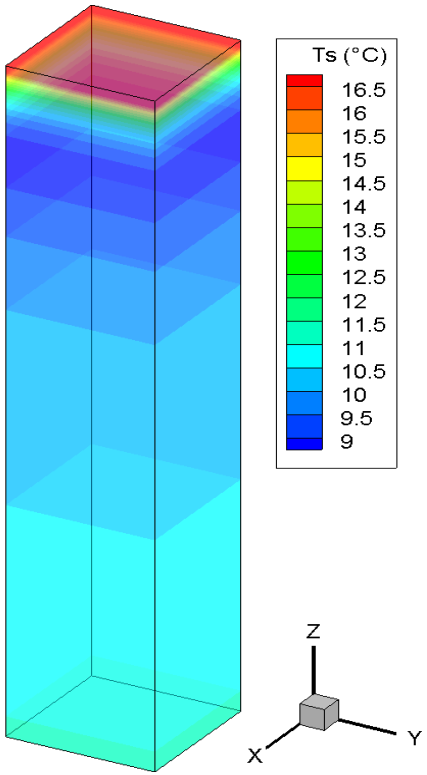

After 3 months

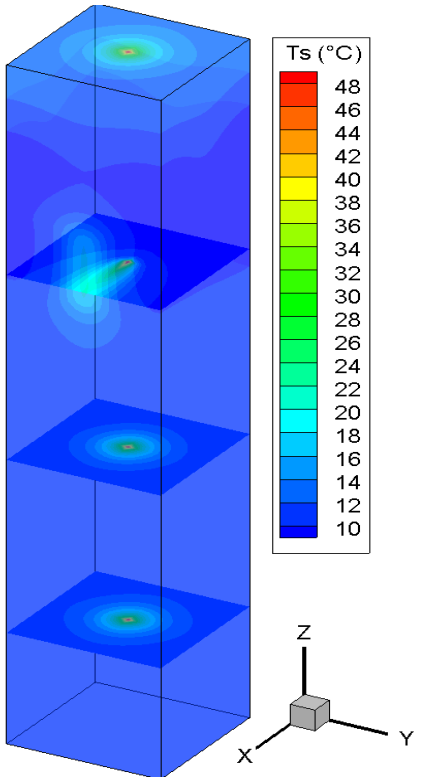

After 7 months

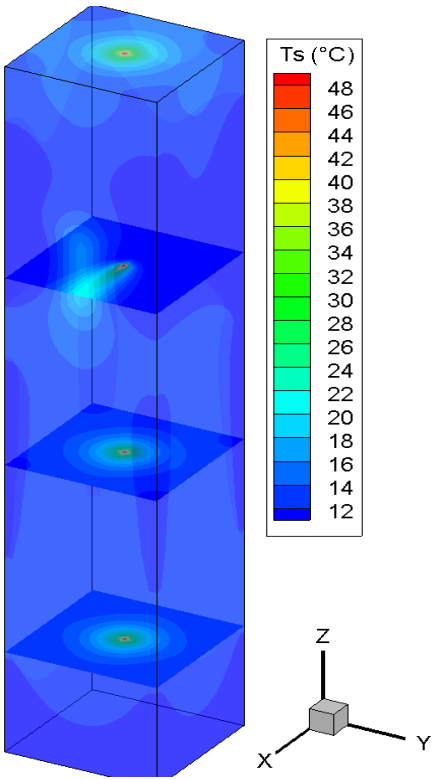

Figure 32 – Charging of borehole heat exchanger for 6 months

RESULTS AND DISCUSSIONS. Numerical results

In numerical studies, charging of one borehole heat exchanger was also considered. Charging was continued 6 months during the summer and inlet temperature was set 65°C (const.). In this study takes into account an aquifer, which velocity of underground flow is 10cm per day. Such studies give opportunity to estimate the distance length of between borehole heat exchangers in BTES system (Figure 32).

Initial state

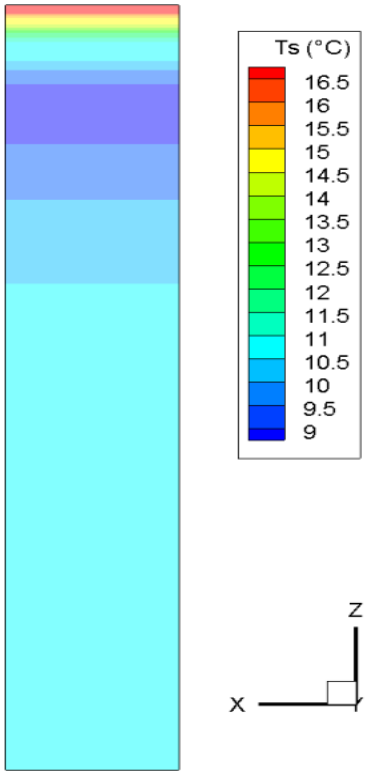

After 3 months

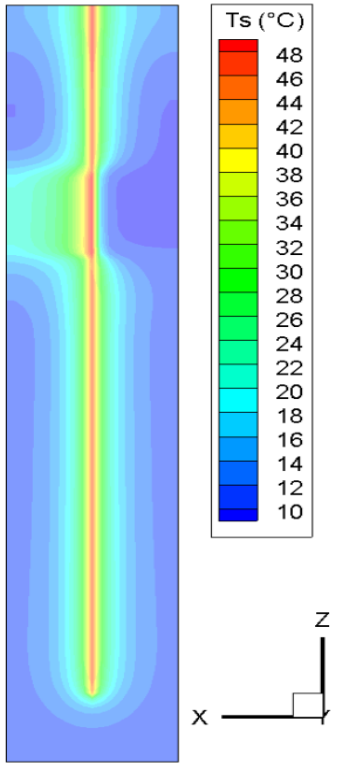

After 7 months

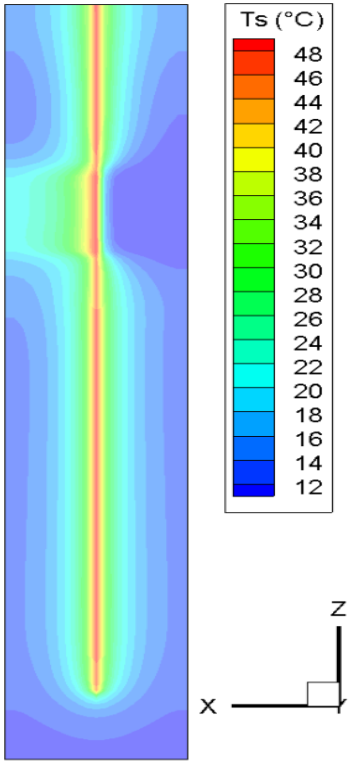

Figure 32 – Charging of borehole heat exchanger for 6 months

RESULTS AND DISCUSSIONS. Numerical results

Numerical computation was carried out for BTES system consisting of 12 borehole heat exchangers. BTES system was charged during the 7 months unceasingly. The temperature at the inlet of boreholes was 70°C and borehole heat exchangers were not connected in series.

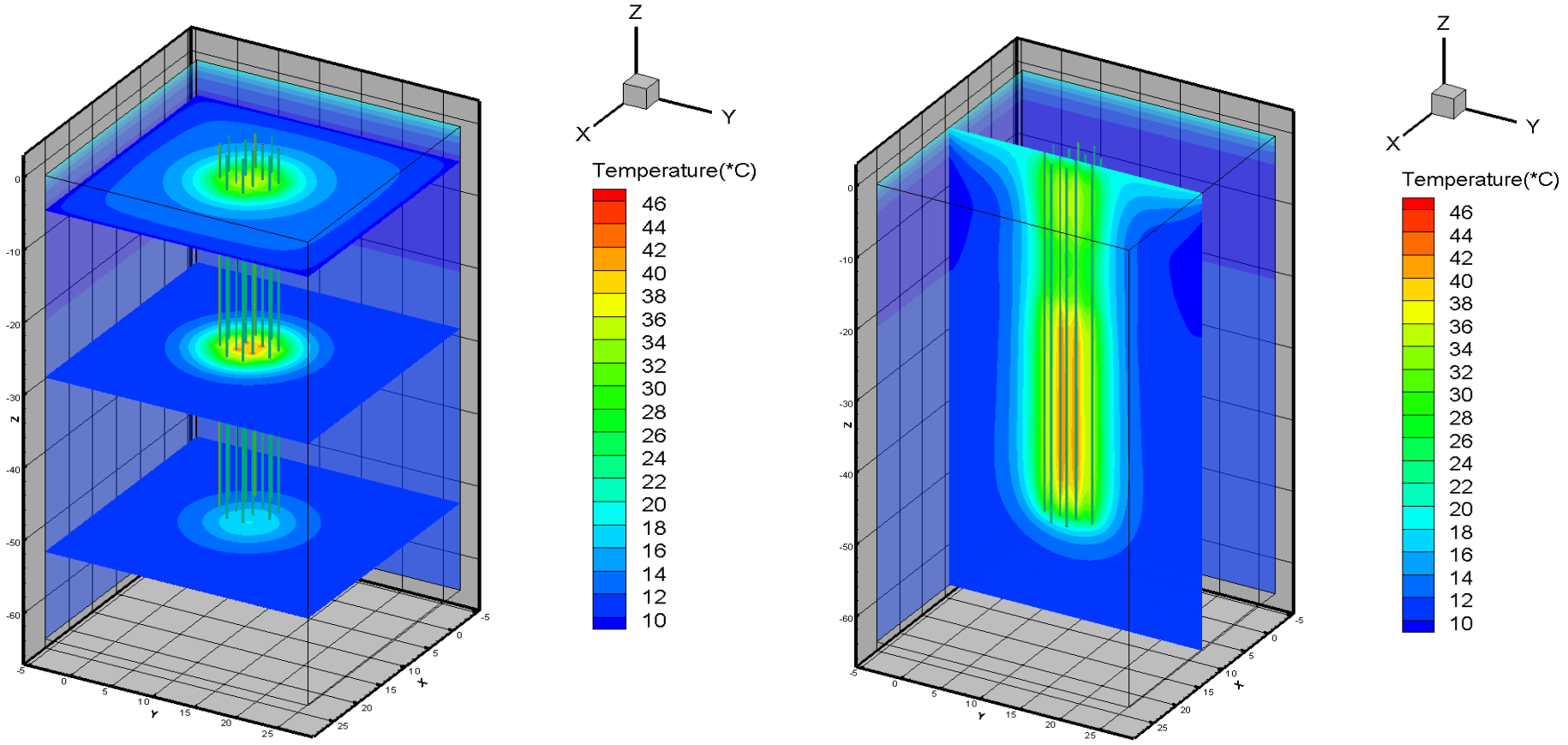

Figure 33 - Temperature field in the BTES system

RESULTS AND DISCUSSIONS. Numerical results

Numerical computation was carried out for BTES system consisting of 12 borehole heat exchangers. BTES system was charged during the 7 months unceasingly. The temperature at the inlet of boreholes was 70°C and borehole heat exchangers were not connected in series.

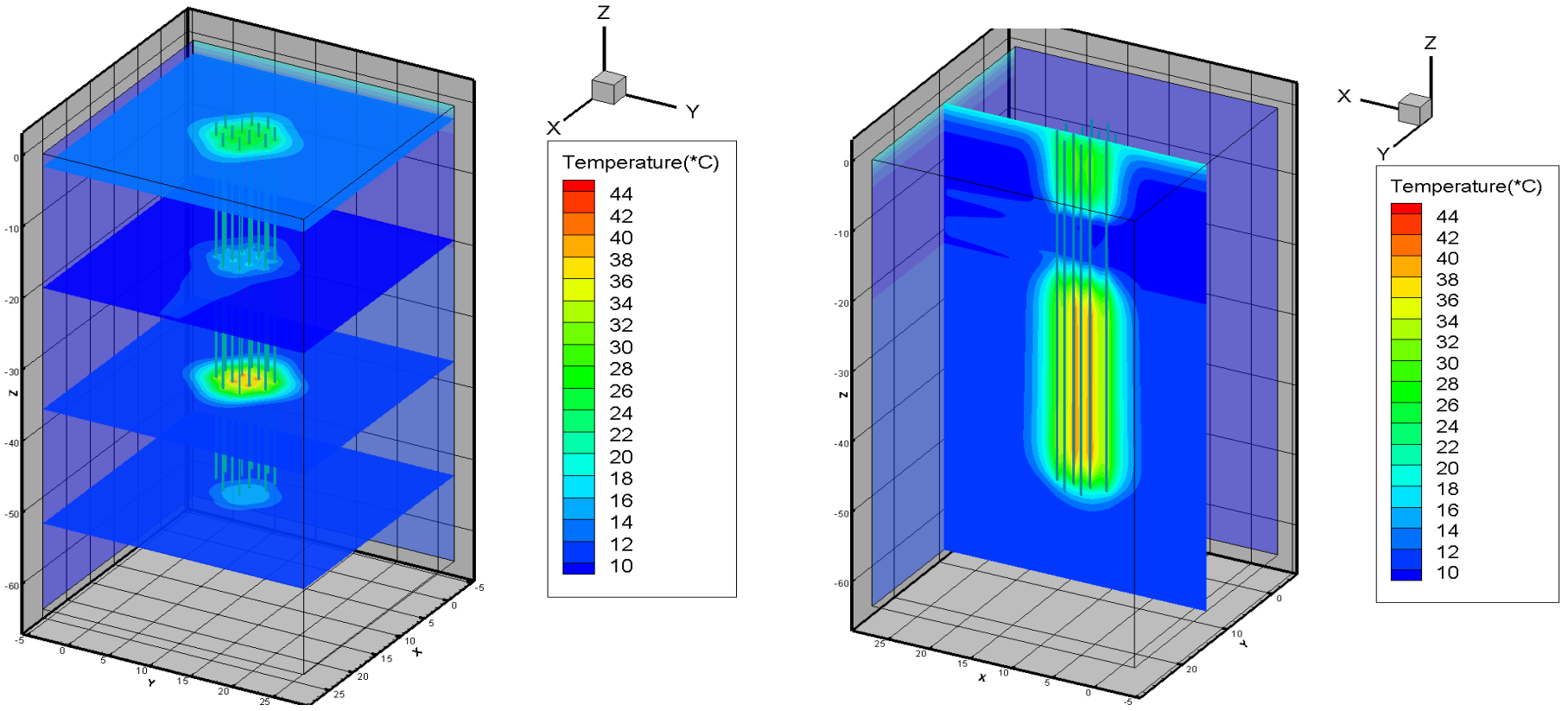

Figure 34- Temperature field in the BTES system

PUBLICATIONS

- T. Amanzholov1, B. Akhmetov2, A. Georgiev3, A. Kaltayev1, R. Popov4, D. Dzhonova-Atanasova5, M. Tungatarova, Numerical modelling as a supplementary tool for Thermal Response Test, Bulgarian Chemical Communications, Volume 48, Special Issue E (pp. 109 - 114) 2016
- T. Amanzholov1, B. Akhmetov2, A. Georgiev3, A. Kaltayev1, R. Popov4, D. Dzhonova-Atanasova5, R. Manatbayev, M. Tungatarova, Installation for thermal response test implementation , 15th "International Scientific Conference" RE & IT - 2016, Smolyan - Bulgaria

Thank you for attention!!!

A NUMERICAL ANALYSIS.
Initial and boundary conditions of the soil

The temperature gradient over the altitude of vertical ground heat exchanger is taken into account to increase the accuracy in the modeling. The initial temperature distribution along the vertical ground heat exchanger was measured before the start of the thermal response test. The results of the measurement are shown in figure.

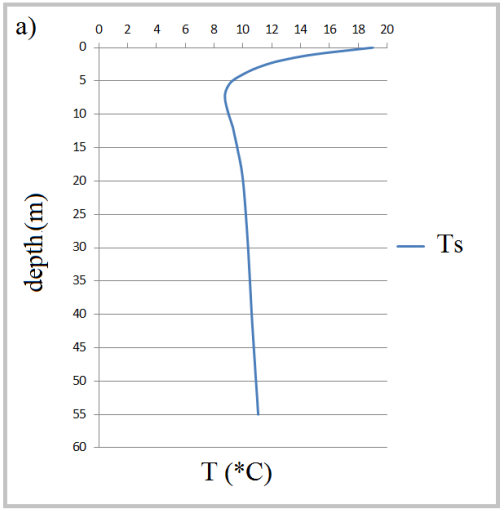

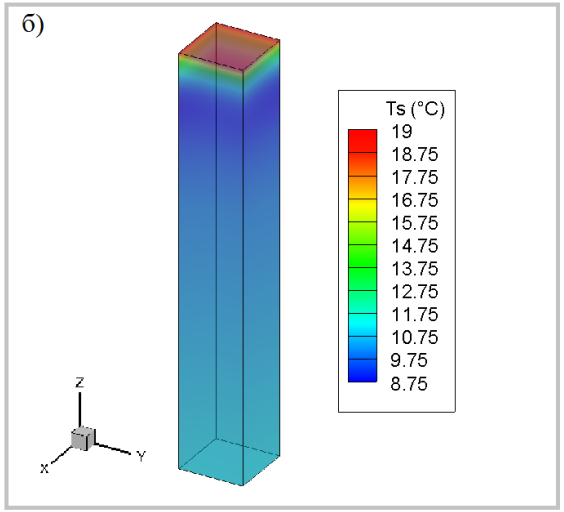

Boundary conditions can be either

$$\lambda_z \frac{dT_s}{dz} n_z = b_{sg}(T_g - T_s) \qquad (1)$$

$$\frac{\partial}{\partial x}\left(\lambda_x \frac{\partial T_s}{\partial x}\right) + \frac{\partial}{\partial y}\left(\lambda_y \frac{\partial T_s}{\partial y}\right) + \frac{\partial}{\partial z}\left(\lambda_z \frac{\partial T_s}{\partial z}\right) + h_{as}(T_s - T_a) = 0 \qquad (2)$$

$$\lambda_x \frac{\partial T_s}{\partial x} + \lambda_y \frac{\partial T_s}{\partial v} + \lambda_z \frac{\partial T_s}{\partial z} + q = 0 \qquad (3)$$